NTNU – Trondheim
Norwegian University of
Science and Technology

Sub-Wavelength Aggregation and Fusion performance experiment

Zekarias Teshome Birhanu

Master of Telematics - Communication Networks and Networked Services (2
Submission date: June 2014
Supervisor: Steinar Bjørnstad, ITEM
Co-supervisor: Raimena Veisllari, ITEM

Norwegian University of Science and Technology
Department of Telematics

Project description

The core of our communication network uses two switching techniques to route information between node devices. Circuit switching is a technique that is proven to have a better quality with guaranteed service, but is also inefficient in resource utilization. Better quality comes from dedicating resources for the duration of a communication session. On the other hand, packet switching uses statistical multiplexing to utilize resources efficiently; this introduces flaws in quality of service.

By combing the best properties of circuit and packet switched networks, TransPacket (www.transpacket.com) has developed a future proofed fusion technology, also known as Optical Migration Capable Networks with Service Guarantees (*OpMiGua*) [1] integrated hybrid network.

In order to provide concrete evidence on the aforementioned best property of fusion technology, in this thesis we will measure performance metrics like latency, latency variation (packet delay variation) and packet loss on live network. The measurement shall be performed in the laboratory of TransPacket in Oslo or in a test bed at UNINETT.

Supervisor: Professor Steinar Bjørnstad, ITEM
Co-supervisor: Raimena Veisllari, ITEM

1) On this thesis, the term OpMiGua, Fusion node, H1 node, and Integrated hybrid optical network node is used interchangeably.

Abstract

The communication network that has connected most part of world's population, and continues to bring more people to the communication grid is being overwhelmed by a vast amount of traffic coming from an increasing number of new services. According to predictions from [1], a threefold increase is expected for the coming five years. This growth trend calls for high performance communication networks.

Although the tremendous bandwidth from fiber supports transport of huge data from one place to another, todays switching technologies provide either deterministic quality in circuit switches or high resource utilization in packet switches. Regard to user applications transported on networks, while some of them require a deterministic circuit switch type of transport, others can be transported better in packet switch that are efficient in resource utilization.

TransPacket Fusion switching [2], a hybrid type of switching integrates both circuit and packet type transport on a single node; hence can support various types of user applications from both worlds. It provides a deterministic circuit transport using dedicated wavelength, and uses the vacant gap on the wavelength to transport a low priority packet without affecting packets that are transported with deterministic quality.

On this thesis, we build on the concept of hybrid switching by aggregating multiple sub-wavelength traffic, which have deterministic characteristics, on a single wavelength. In addition to that, we demonstrate how the vacant gaps from the aggregated traffic can be used to transport low priority packet traffic.

Several experiments have been performed on a network set at UNINETT with Fusion prototype hybrid nodes from TransPacket. The results from the experiment show that: Fusion node can provide the required strict quality of service to the aggregated sub-wavelength circuits while, at the same time, increase resource utilization by injecting low priority traffic on vacant gaps.

Acknowledgments

I would like to thank my supervisor Professor Steinar Bjørnstad for his support and advice; I would also like to thank Raimena Veisllari, my co-supervisor, for guiding me throughout my thesis, and help me to think and work independently. I want to thank Kurosh Bozorgebrahimi and Arne Oslebo for the support they provide at UNINETT.

I also like to extend my gratitude to the Department of Telematics, especially Mona Nordaune, Laurent Paquereau and Pål Sæther.

Sincere thanks to my family for all the good wish and encouragement all along my life; special thanks go to my aunt Azeb Abebe. It has been very important to have Miheret nearby, thank you for the continuous presence and care.

Contents

List of Figures

List of Tables

Abbreviations

ATM	Asynchronous Transfer Mode
BCP	Burst Control Packet
CWDM	Course wavelength Division multiplexing
DCF	Dispersion Compensating Fiber
DMUX	Demultiplexer
e2ed	End-to-end delay
FDL	Fiber Delay lines
FEC	Forwarding Equivalence Class
FIFO	First in first out
1 GE	Gigabit Ethernet
10 GE	10 Gigabit Ethernet
GST	Guaranteed Service Traffic
IHON	Integrated hybrid optical node
ITU-T	International Telecommunication Union-Telecommunication Standardization Sector
LSP	Label Switching Path
MAN	Metropolitan area network
MEMS	Microelectromechanical systems
MPLS	Multiprotocol Label Switching
NGS	Number of GST streams

NTNU	Norwegian University Science and Technology
O/E/O	Optical-Electronic-Optical
OBS	Optical burst switching
OCS	Optical circuit switching
OpMiGua	Optical Migration Capable Networks with Service Guarantees
OPS	Optical packet switching
OTN	Optical Transport Network
PDV	Packet delay variation
PLR	Packet loss ratio
QoS	Quality of service
SDH	Synchronous Digital Hierarchy
SM	Statistically multiplexed
SONET	Synchronous Optical Networking
SSH	Secure Shell
TDM	Time Division Multiplexing
TL	Total load
VLAN	Virtual Local Area Networks
WDM	Wave division multiplexing
WRON	Wavelength routed network

Chapter 1

Introduction

1.1 Overview

As social beings dwelling on planet earth we have developed several ways of passing information amongst ourselves; these methods have been the main driving force for our thriving civilization. The ambition of extending our communication ability in broader geographic areas has led to the development of extensional devices that are capable of transmitting information in long ranges.

Starting from using fire as a tool of signaling to our nearby neighbors, we have digitized our information, used different kinds of communication mediums, unplugged ourselves from wires using wireless devices, and introduced different techniques of sharing resources to quench our need of passing information without the barrier of geographic terrains.

By processing our voices, pictures, writings into forms that can be manipulated by man-made devices, it was possible to do what was impossible before: long range communication; in different periods of time we have identified and developed devices that are capable of aiding the only medium of communication we ever had, air.

We are also successful in building big networks that are efficient in sharing resources based on the concept of circuits; circuit and packet switching are two ways of routing information inside our communication networks.

Generally, real-time communication requires a dedicated circuit setup from sender to receiver in order to offer guaranteed quality, minimum delay and no loss; delay and loss in such type of applications disrupt smooth communication. If the communication is of type that can be delivered with flexible Quality of Service (QoS), information can be fragmented, tagged with source and destination address, and transported on packet switches similar to how we utilize our postal systems.

Circuit switches provide guaranteed service, but they are poor in resources utilization; therefore, it was necessary to develop switches that are efficient in managing resources: packet switches provide that on the expense of quality of service [3].

The best effort quality from the packet switches is not suitable for services that require a guaranteed quality. Consequently, several approaches have been used to make packet switched networks capable of handling several services with different QoS requirements.

Yet to integrate voice, video and data transport in a converged network architecture, better resource exploitation techniques are required. For this reason, it is necessary to resort to hybrid networks that integrate merits of both circuit and packet switching.

On this thesis, we measure the performance of integrated hybrid optical network nodes, also known as Fusion; performance measurement will mainly focus on packet delay variation (PDV), packet loss ratio (PLR) and end-to-end delay (e2ed).

1.2 Motivation

The integration of fiber optics to communication networks was a successful leap in providing a vast amount of bandwidth; moreover, currently, researches are exploring more in the field of optics to incorporate optical technology deep into communication networks. Fusion node, a hybrid optical technology, is the output of such research that combines the best properties of circuits and packets technology.

Suppose we have three customers who would like to get hard quality access to a network. The circuit switching approach offers each user a dedicated light-path/circuit/wavelength with the required hard QoS; however, light path remains idle when users are not using it. In case a new customer asks for a best effort or hard QoS access, another wavelength should be assigned. Although hard quality is guaranteed, managing scarce resource – wavelength - in this manner is inefficient.

On the other hand, if packet switching is used, the available resource is shared among the three customers using statistical multiplexing; this leads to a better resource utilization, but is not suitable for traffic types that require strict QoS.

Aiming to support various service requirements from several application types, TransPacket fusion node introduces two classes/types of traffic: Guaranteed Service Transport (GST) and Statistically Multiplexed (SM) traffic. GST traffic is transported on a dedicated light path over wavelength routed network (WRON) with guaranteed QoS. The gaps between GST packets are utilized by low priority SM packets. This has enabled the fusion node to provide guaranteed QoS for GST traffic independent of the added SM traffic. In addition, the added SM traffic maximizes the utilization of the light path.

If we consider the three customers' scenario for the hybrid technology, whenever a new customer requires best effort service, the fusion node utilizes the gaps from the three customers' light paths to handle the new customers' traffic. This ability of fusion node has been proved to work through several experiments, then again how would a fusion node handle if the new customer requires a guaranteed QoS? This is another scenario that is going to be studied on this thesis.

The fusion integration technique can be further used to aggregate multiple GST streams together with SM traffic on a provisioned single light path. Following the raised question from the above example, when a new customer requires hard QoS, time slots can be used to aggregate several GST channels within a provisioned GST wavelength. If unutilized gap is found between the aggregated GST packets, SM packets can be inserted.

Fusion node aggregates multiple incoming sub-wavelength GST traffics on a single wavelength using data containers; packets of a sub-wavelength traffic are placed in their containers after the inter-packet period is extracted. This period maintains the gap between the packets, and later used at the destination to reconstruct the packet stream after de-aggregation.

1.3 Objective

In order to cope up with the fast growing internet traffic that comes with the proliferation of new network services, technologies that are capable of utilizing the available resource are needed. The objective of this thesis is to demonstrate how TransPacket fusion node can back this requirement by:

- Aggregating multiple circuit quality sub-wavelength GST traffic on a single wavelength, and
- Add more SM traffic between gaps of GST traffic, hence increase utilization of existing network infrastructures

1.4 Thesis outline

This thesis is organized in seven chapters, the first three chapters focus on background work, and introduction to hybrid optical switching in particular TransPacket H1 hybrid switch, and related works. The fourth chapter describes the experimental approach followed on this thesis. On Chapter 5, results from the experiments are presented; which are further discussed and analyzed in chapter six. Conclusion is given/drawn in Chapter 7.

Chapter 2

Background

The focus of this thesis is presenting concepts and techniques that are related to performance of communication networks. This chapter will introduce communication network elements, discuss about technical concepts of multiplexing and switching, and finally will present parameters that are used to measure the performance of communication networks.

2.1 Elements of communication network

Network links, switching equipment (nodes) and software layers (comprising protocols and applications) implemented at the switching and end-nodes are the main building blocks of high-performance networks. Users of the network, regardless of their distance, can use these components to transfer information between themselves. The network structure, shown in Figure 2.1, depicts the end-nodes, links, and switches.

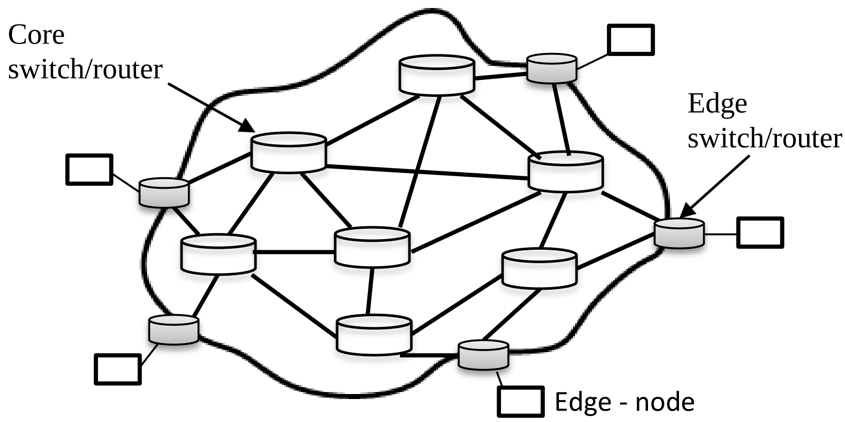

Figure 2.1 Network elements.

End nodes, represented as squares, are sources and sinks of information used by users as an access to the network; personal computers, mobile phones and printers are examples of end node.

Information from one end node to another end node is transported by the path provided by links. Copper wires, optical cables, are some examples of links.

Several incoming and outgoing links are connected by switches; switches are used to route data flows from one incoming link to another outgoing link. As can be seen from figure 2.1, while edge switches connect end-nodes to the network, core switches are interconnected to switch information to the destined users; the two kinds of switches are depicted as grey and empty circular cylinders respectively.

For several reasons, it is not efficient to establish a one-to-one connection between users; cost can be mentioned as one reason. Instead, the desired connectivity is achieved by using shared communication resources at a cost of fair degradation in quality of service. Multiplexing and Switching are two main techniques that are widely used in sharing the common communication infrastructure. The following section gives further description on these two techniques [4].

2.2 Multiplexing and Switching

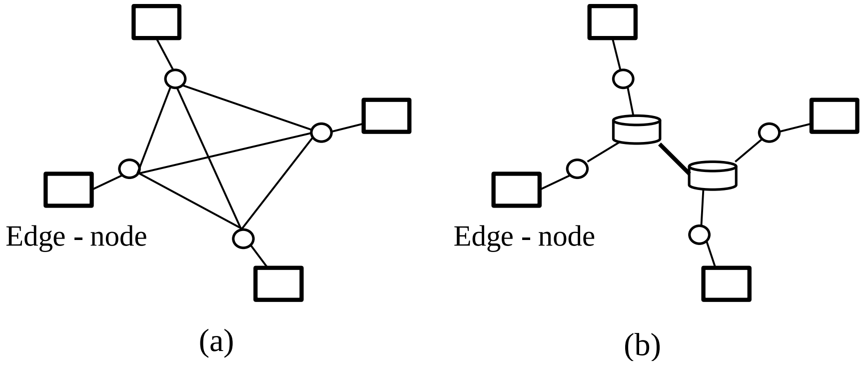

Figure 2.2 Network connection between edge nodes (a) a fully connected network (b) multiplexing and switching in networks.

Figure 2.2 (a) illustrates use of dedicated links between two pairs of users. Links are dedicated; therefore it provides a high quality as the customer traffic is not competing for resources with other customers' traffic. However, link remains idle when users are not using it; hence it is inefficient in link utilization. Such kind of networks waste resources, and introduce an increase in cost with number of users. Figure 2.2 (b) shows how sharing of resources among users made possible by switching and multiplexing techniques. Switches can multiplex data coming from different users and route to the destined users. Since number of links and switches increase less rapidly with the number of users, cost is reduced compared to using dedicated links scenario.

2.2.1 Multiplexing

Multiplexing is a technique that is used to combine N incoming channels and transmit on one outgoing channel. On the reverse technique, i.e. demultiplexing, the multiplexed incoming channel is separated into individual N outgoing channels. Although there are several known multiplexing techniques, this section discusses only the ones related to this thesis, namely Time Division multiplexing (TDM), Wave division multiplexing (WDM) and Statistical Multiplexing.

2.2.1.1 Time Division Multiplexing

TDM is a way of dividing time into intervals called frames, each frame is further divided into N timeslots: slot 1, slot 2… slot N. The operation of TDM multiplexer is depicted on Figure 2.3. It starts by reading the data bits of incoming channel into separate first in first out (FIFO) buffer, these buffers are then read sequentially for a period of slot time by the multiplexer, e.g. data bits from buffer 1 into slot1, buffer 2 in to slot 2, etc. Demultiplexing is done by reading framing patters that are inserted at the beginning of each frame to indicate the start of a frame

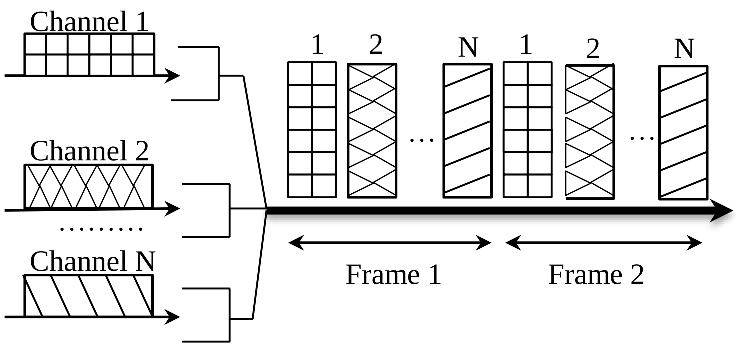

Figure 2.3 Time Division multiplexing adapted from [5].

2.2.1.2 Statistical multiplexing

Statistical multiplexing is an efficient way of multiplexing when the incoming traffic is bursty. In TDM incoming channel gets a fixed fraction of time on the outgoing channel capacity. However in case of statistical multiplexing, the higher the rate of the incoming channel the larger fraction of time it gets on the outgoing channel, i.e. the outgoing channel is expected to have a capacity that is equal to the sum of the average data rates of the incoming channel. Each packet should have source/channel identifier and packet delimiter; making the implementation of multiplexer difficult. This makes SM to have a larger overhead than TDM.

While Voice, fixed-rate video, sensor signals are constant bit rate traffic which use TDM, database transactions and variable bit rate videos generally uses Statistical Multiplexing [5]. That is why TDM is more effective in our telecommunication networks, and statistical multiplexing is in networks of computers.

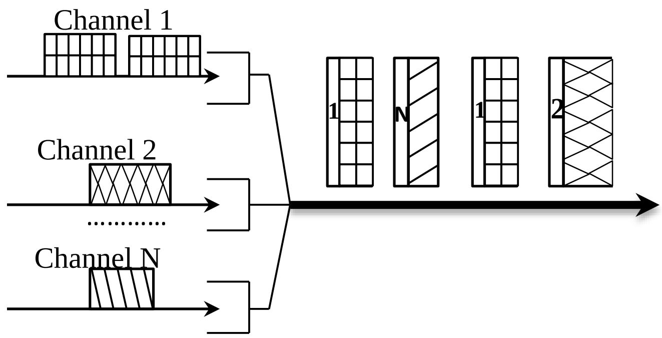

Figure 2.4 Statistical multiplexing adapted from [5].

2.2.1.3 Wave division multiplexing

WDM is a multiplexing technique that is used in fiber optics. In the low-loss wavelength region of an optical fiber a bandwidth of 40 THz is available [6]. WDM divides the optical spectrum into several wavelength channels, each capable of carrying a data channel; therefore using WDM, higher fiber utilization can be achieved. Neighboring wavelength channels can be used to transport different kinds of traffic side by side, like Ethernet [7], Synchronous Digital Hierarchy (SDH)/ Synchronous Optical

Networking (SONET) [8] [9], and Optical Transport Network (OTN) [10]. In addition, different bit rates up to 10 Gb/s can be used; this makes WDM protocol and bit rate independent.

2.2.2 Switching

Large networks are built from different network components that are connected by switches (routers and bridges are also network components that use switches); due to this functionality of switches, as a glue to connect network components, communication networks are commonly named switched networks. Switched networks have make connection to any location at reasonable cost [5].

In today's networks, circuit and packet switching are two main ways of setting up a path (switching) through a network; in addition, hybrid switching is a recently introduced technique to switch data, the following sub-sections discuss these concepts.

2.2.2.1 Circuit Switching

When using circuit switching, data is moved between two end users by setting up a unique path reserved for the duration of the communication session. Dedicating resource works well for constant bit rate traffic because the channel is always utilized by the data. However, when the traffic is bursty, the dedicated channel remains idle in the absence of traffic; this is the case, even, when other users sharing resource are waiting for channel.

In circuit switching communication takes place based on the following three main phases.

1. **Connection establishment:** on this phase a path/connection is set prior to transferring data by exchanging information about available resources among switches; when a path is available this information is passed to the end user.
2. **Data transfer:** on the second phase, the already set up path on the first phase is used to transfer data between users.
3. **Connection tear down:** the last phase is tearing down/freeing the connection. This is done by intermediate switches at the completion of data transfer.

Switching in circuits can be performed in both electrical and optical domains. Transmission of high bandwidth multimedia applications such as video-conferences, online gaming and web-television streaming in core networks, with lower cost, is possible using multiplexing technique in optical domain (WDM). Moreover, by switching and routing in the optical domain we can reduce switching and routing cost, and hence achieve cost-effective optical core networks [11].

Optical circuit switching

In the early age of telecommunication, switching was done by human operators that were replaced by mechanical switches, and latter advanced to electrical switches.

Today, even replacing the matured electrical switches is becoming inevitable. When working with electronic switches, the optical signal on WDM has to be converted in to electrical signal for electrical processing and then converted back to optical for further transmission, this Optical-

Electronic-Optical (O/E/O) conversion limits the capacity of the switches, not only that it introduces additional cost.

Optical circuit switching (OCS) network, also known as WRON, works by setting up a dedicated light path (wavelength) between edge nodes of the core network. Switching technologies such as Microelectromechanical systems (MEMS) [12], thermal optical switching [13] are used in OCS. Implementing optical switches takes the speed of switching in millisecond range [14].

Being a type of circuit switching technology, WRON is not optimal in link utilization, but it can be improved by introducing statistical multiplexing in a switching technique called optical packet switching (OPS) and optical burst switching (OBS).

2.2.2.2 Packet Switching

When using packet switching, data is segmented into fixed or variable sized packets depending on the type of protocol used. Datagram and virtual circuits are two approaches to switch packets [15].

When using datagram switching, routing information that is used to get to the destination is carried by the packets, and packet processing is done independently on each packet; as a result connection establishment phase is not required. Each packet can use different paths to reach to their destination with an advantage of dynamical re-routing during faulty communication.

When using virtual switching, end users transmit data using a unique path that is similar to circuit switching. Nevertheless, it is different from circuit switching that idle channels can be utilized by other users. One example of virtual switching is Asynchronous Transfer Mode (ATM). ATM was chosen by many carries for its excellent performance, traffic engineering, and cost-effectiveness in multiplexing internet traffic over ATM (in IP over ATM model) by the mid-1990s. However, later, the simpler mechanisms of packet –oriented traffic engineering, multiservice functionality, and the greater scalability from Multiprotocol Label Switching (MPLS) were found better viable solutions. [16]

MPLS has made the complex next-hop decision making process in IP routers simpler by using a decision mechanism based on labels. A group of flow packets that require the same traffic engineering requirement are assigned in the same table called Forwarding Equivalence Class (FEC), and FECs are given a specific label. MPLS networks use Label Edge Routers at the ingress of the network to label incoming IP packets, and sent out on path called Label Switching Path (LSP). Label Switching Routers found on the LSP forward packets by swapping the labels of incoming packets with a new label. [17].

When it comes to optical domain, packet switching is done by isolating packet forwarding from packet switching in OPS and OBS.

Optical packet switching

In OPS, the forwarding decision is done by looking into the header information that is transmitted simultaneously with the payload; here, the same wavelength is used for both the header and the payload. Figure 2.5 (a) show an OPS packet format. Packets undergo hop by hop processing and forwarding until they reach their destination node.

Although, currently, packet headers are processed electronically due to immature optical processing technology, an optical domain processing, forwarding and buffering is required in OPS. Electrical processing is done by extracting the header, and converting it into electronic domain while the payload is delayed using Fiber Delay lines (FDL) [18]. Because of statistical multiplexing in OPS, resources utilization is better than WRON.

Optical Burst Switched networks

OBS aggregate and transmit packets, in the form of bursts, from access networks to the OBS network based on their destination, and service class [11].

The OBS network forwards packets to their destination optically in a hop-by-hop manner. Forwarding is done based on the header information, e.g. as depicted in figure 2.5 (b); a separate packet called Burst Control Packet (BCP) that precedes the burst is used for this purpose.

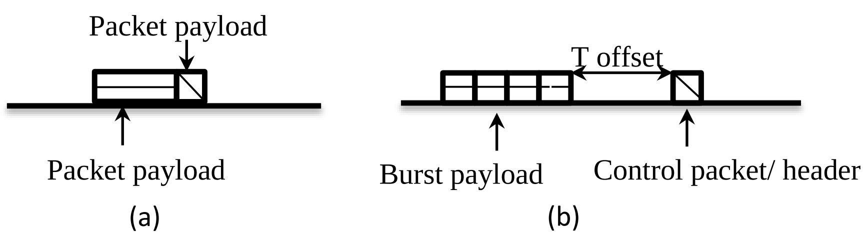

Figure 2.5 Packet structure (a) OPS (b) OBS [11].

2.2.2.3 Hybrid Switching

Hybrid switching is a third type of switching technique that was introduced recently. Three kind of hybrid networks have been proposed at different times incorporating the merits of circuit and packet switched networks: client-server, parallel and integrated. The following section will give a brief description of this three techniques [19].

Client-server hybrid optical networks

Figure 2.6 shows a client-server hybrid optical network with two adjacent layers. The lower layer which serves as a circuit switched server sets up a virtual topology for the upper client layer. Traffic is aggregated at the edge of the core network by the OBS or OPS node, which are interconnected by direct light path in the circuit switched network. The circuit switched server layer transport optical bursts/packets which are only switched in the client layer nodes. The number of burst-mode-capable switch interfaces can be reduced by directing traffic in light paths and this offloads the OBS and OPS nodes.

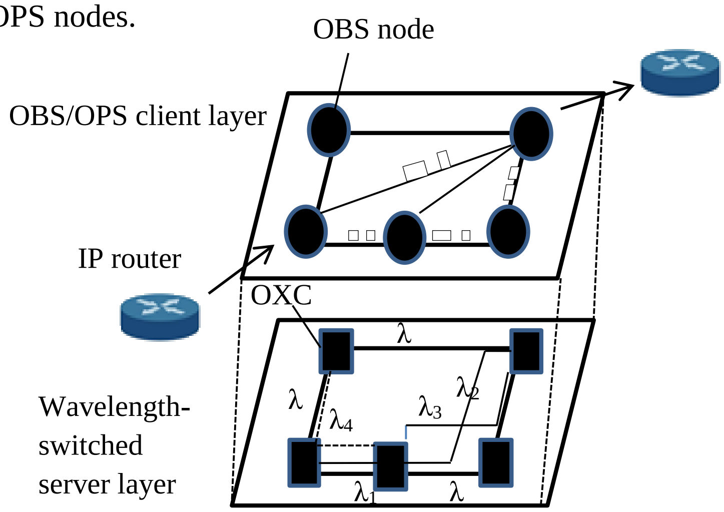

Figure 2.6 Client-server hybrid optical networks [19].

Parallel hybrid networks

Parallel hybrid networks use two or more parallel optical layer networks. These layers offer different transport services that an intelligent edge node can combine or use separately with the aim of providing an optimal service for customer requirements. Figure 2.7 depicts a parallel hybrid optical network.

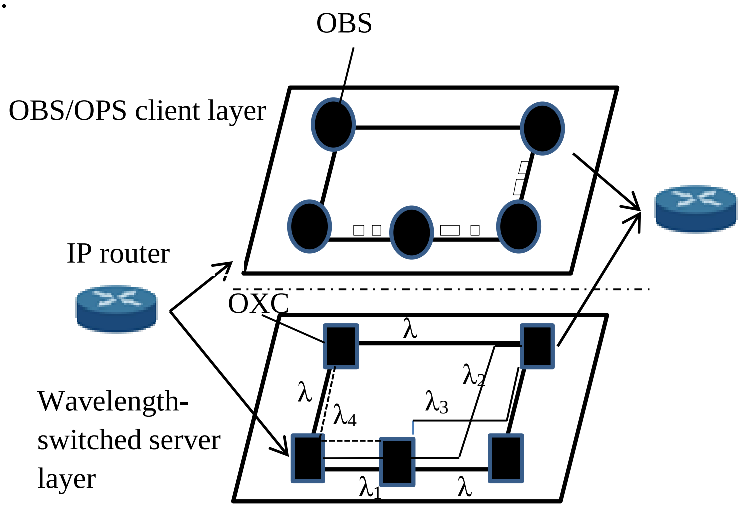

Figure 2.7 Parallel hybrid networks [19].

Integrated hybrid optical networks

Integrated hybrid optical network (IHON) integrates the circuit and packet optical switching; the same bandwidth resource is shared among the integrated technologies. Figure 2.8 shows IHON architecture with each node built from a circuit and packet switched technology. Unless in case of congestion where by packet switched mode is used, usually, the end-to-end light path will transmit packets; using the end-to-end light path avoids packet processing by subsequent nodes. QoS is another differentiation mechanism to switch between switching technologies.

IHON provides optimal service from resource point of view. The theme of this thesis is a study on the performance of OpMiGua which is a type of IHON node.

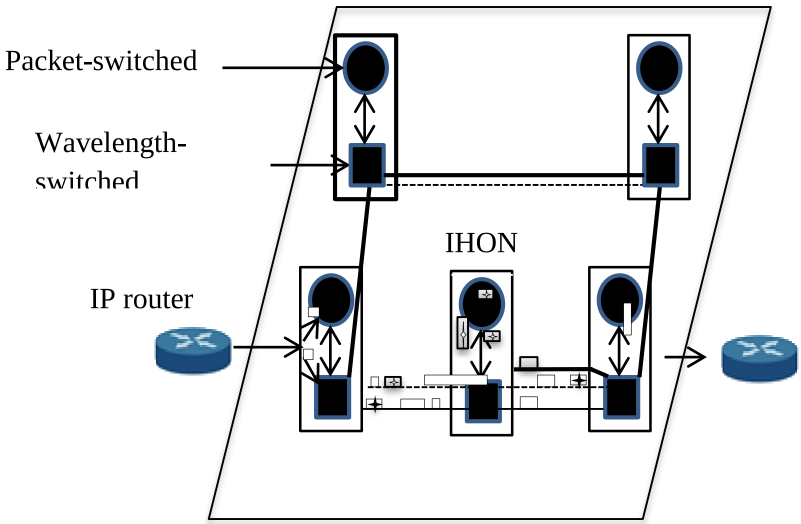

Figure 2.8 Integrated hybrid networks [19].

2.3 Network performance parameters

High performance network is defined in [5] as “a communication network that supports a large variety of user applications and that is scalable”.

Supporting many applications can be achieved by providing high speed and low delay transmission, allocating resources based on application requirement, and providing flexible network organization and management.

Networks can be scalable by accommodating a growing number of users without degrading the offered performance; the growing number of users is handled by providing interconnectivity of networks over a growing span.

2.3.1 Techniques for Performance Analysis

In the scientific community, there are three way of evaluating the performance of a network: 1) measurement, 2) analytic modeling and 3) simulation [20].

The most fundamental approach is measurement which can be done either in software/hardware or in hybrid manner. This approach is costly, and involves a great deal of time.

Analytical modeling is a two-step process: first the mathematical model is developed and the model is solved in the second step.

Simulation imitates certain important aspect of a real system by designing a model. It is a cheaper method of performance analysis.

2.3.2 Performance measures

Together with the performance analysis techniques, one of the following six metrics can be used for measuring the performance of communication networks [20].

1. **Capacity**: It is the quantity of traffic the system can accommodate, and is measured by Erlangs, bits/s, or packet/s.
2. **Throughput**: It is the measure of the quantity of traffic that reach at the destination successfully.
3. **Queue length**: It is a measure of the required length of a buffer.
4. **Delay**: It is a measure of the time to transmit the traffic from source to destination. Delay can further be classified into four components: processing delay, queuing delay, transmission delay and propagation delay [21].

The processing delay is the amount of time it takes to locate packet's next route from header information; processed packets are then buffered in a queue, queuing delay, until the packet is sent to the next route. After this time, the packet should be transmitted to the destination using the provided link, the amount of time that is needed to push/transmit packets from the node to the link is called the transmission delay; it is calculated by dividing packet length (L), with the link rate (R), i.e. L/R. The propagation delay is the amount of time it takes for packets that are pushed on the link to propagate to the destination node.

5. **Loss probability**: It is a measure of the probability that traffic is lost.
6. **Jitter**: It is a measure of the variation in packet delay.

On this thesis, we have used the first, measurement, performance analysis technique using the last three performance metrics mentioned above.

Chapter 3

Fusion Networks

In order to transport information from one place to another, traditionally, fiber optic networks have been using circuit switching techniques in their networks. Even though circuit switched networks are capable of providing synchronization support, low latency, and low latency variation, they are not efficient in using the shared resource. On the other hand, by introducing statistical multiplexing, packet switched networks has proved to be efficient in resource utilization; therefore enabling higher throughput with lower cost.

The high efficiency and low cost gain from the packet switched networks has led to the replacement of circuit switched core with packet switched core [22]. However, pushing the packet switch to the core of communication networks call for an efficient way of transporting several communication services with different QoS requirement. For instance, some services demand circuit switched networks QoS: low latency, low latency variation, and transport of synchronization. In addition to that, since routers found in the core of packet switched network are passages to a larger part of the traffic in the network, processing the through-passing traffic requires costly high performance routers.

Aiming to support the requirements from several communication services, different improvements have been made to the packet switched networks. Despite their success in providing the required qualities, they have introduced complexity in the hardware and software structure, as a result increased the cost. This has made the operational and capital cost of these techniques expensive.

That is why it is necessary to introduce the concept of hybrid switch networks, that integrates both circuit and packet switch technologies, to provide support for various services. The first section of this chapter focuses on the basic principle of fusion node, how it operates, packets are scheduled and how free time-gaps are detected. On the second subsection, we will discuss about sub-wavelength aggregation in fusion nodes, and finally previous works related to this thesis is presented.

3.1 Basic principle of Fusion technology

In chapter 2 we have discussed the merits of both circuit, packet and hybrid switching technologies in regard to their applications with various network service requirements. Furthermore, we have pointed out both circuit and packet technologies can be used as optimal solutions for networks with different requirements.

Fusion nodes are developed from the demand for optimal converged service; both guaranteed service from the circuit technology and efficient resource utilization from packet switching technology are supported by the hybrid fusion switching technology.

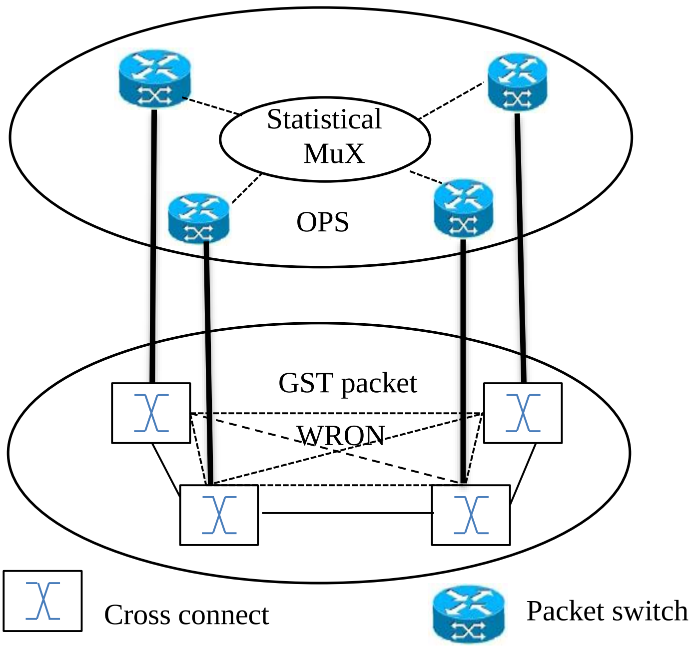

Figure 3.1 Fusion node model, the bottom layer represents WRON a transport for the GST traffic and the upper layer is the packet switch layer transport for SM traffic [23].

A model of TransPacket fusion node is shown in figure 3.1. The hybrid structure transmits the Guaranteed Service Transport traffic in a Wavelength routed optical network which offers constant, short switching delay, and packet delivery without loss or reordering. This allows the GST packets to bypass the packet switches, and hence offloads traffic from packet switch layer [23].

Unlike GST, Statistically Multiplexed traffic should pass through the packet switch layer, buffered in a queue, and wait to be scheduled by SM scheduler until a fitting vacant gap between GST packets is found. The fusion node uses Virtual Local Area Networks tags (VLAN) tags to classify traffic, as GST and SM [24].

3.1.2 Fusion node operation

Figure 3.2 and 3.3 below shows the current interfaces and internal operation inside the TransPacket fusion node respectively. As can be seen in Figure 3.2, the fusion node has ten 1 GE interfaces (ge0 – ge9) and two 10 GE interfaces (Xe0 and Xe1) [25].

The fusion node's internal operation is illustrated by figure 3.3. In order to explain the operation of fusion node, the figure is depicted with three 1 GE input ports (ge 7 – ge9) as SM ports, and one Xe input port (Xe0) as GST. The second Xe port (Xe1) is used as an output port.

The fusion node first classifies the incoming traffic into GST and SM traffic. After the incoming traffic is identified and labelled at the input port of the node, while the GST traffic bypass the packet switch, the SM traffic is dropped to the packet switch by the SM Demultiplexer (SM DMUX).

The dropped SM traffic stay inside a queue buffer, and is processed according to the header information. A separate queue, the same size as the number of input SM streams is assigned to the incoming SM packets, hence for this example three separate queues; in doing so it is possible to increase the number of SM packets that can be added between vacant GST packets.

The gap between the GST packets departing to the output port is measured, using the GST gap detector, and passed to the SM packet scheduler. The scheduler will schedule after it scans for SM packets, in the queue, that can fit the measured gap between the GST packets. Thus, using this intelligent technique, the fusion node increases link efficiency of the underutilized circuit switched traffic (gaps between GST packets) with best effort SM packets.

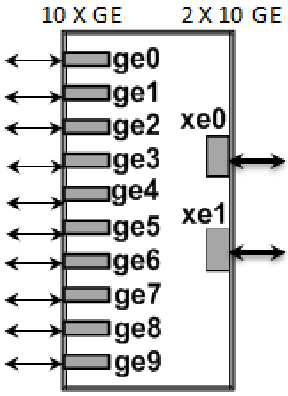

Figure 3.2 Fusion node interface, ten 1 GE ports (ge0- ge9) and two 10 GE ports (xe0 and xe1) [25].

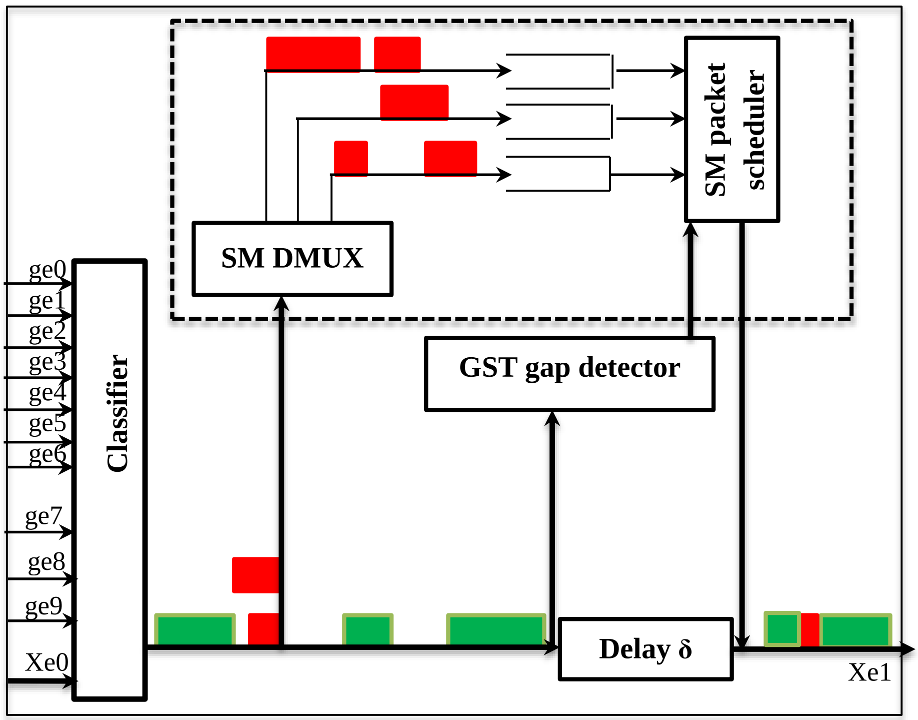

Figure 3.3 Internal operations of fusion node; the figure is used to explain the operation of fusion node, and is depicted with three 1 GE input ports (ge 7 – ge9) as SM ports (red packets), and one Xe input port (Xe0) as GST (green packets). The second Xe port (Xe1) is used as an output port.

In order to prevent pre-emption of SM packets by GST packets, GST packets go through a deterministic delay δ equivalent to the maximum length SM packet service time [24].

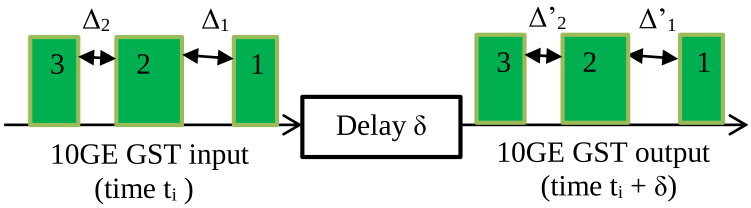

Figure 3.4 Delay experienced by all GST packets is the same, therefore the inter packet gap remains constant; adapted from [24].

Figure 3.4 shows how the inter-gap time between GST packets remains constant after the GST packets pass through the delay component. Δ_i represents the inter-packet gap time between two GST packets; because all GST packets will be delayed to a time equivalent to δ, the gap between the GST packets will remain the same at the output, i.e. $\Delta_i'=\Delta_i$. This implies PDV is not added to the circuit traffic by the fusion node.

3.1.2 Scheduling in fusion node

Figure 3.5 (a) and (b) shows a depiction of scheduling technique used in packet switches with non-pre-emptive priority and in fusion nodes respectively. When a priority scheduler is used, the scheduler gives priority to the highest propriety packets. However, if the queue for high priority packets is empty and a lower priority queue has packets to send, packets will be scheduled from there. In such kind of scheme if a packet with high priority arrives when transmitting the low priority, it will be forced to delay until the transmission is complete. This introduces packet delay variation which fusion nodes avoid [24].

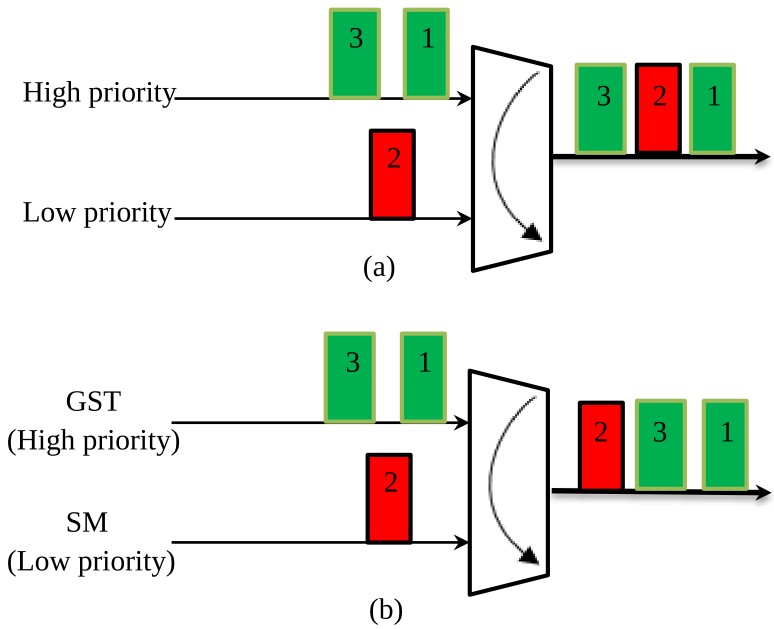

Figure 3.5 Scheduling comparison (a) scheduling in non-pre-emptive priority scheduler, (b) scheduling in fusion scheduler [24].

3.1.3 Detection of free time-gap

A round robin gap filling scheduling algorithm is used to fill the gaps of GST packets on the underutilized light path. The gap measurement starts when GST packet comes in to contact with the delay line; a monitoring module found on the delay line senses the arrival and exit time value of the GST packet, and these values are used to calculate the gap between two consecutive GST packets. Then, the calculated value is sent to the scheduler to schedule the appropriate SM packet from the queue into the vacant gap.

The following steps and figure 3.6 summarize the algorithm that detects the gap between GST packets.

Table 3.1 Notations used to describe the gap scheduling algorithm.

Output channel	λ_w
Arrival time of GST packet i to the delay line of output channel λ_w	$T_{a,i}^{w}$
Arrival time of GST packet i + 1 to the delay line of output channel λ_w	$T_{a,i+1}^{w}$
The service time of GST packet i, the time it takes the packet to enter to the delay line completely	$T_{s,i}^{w}$
Exit time of GST packet i to the delay line of output channel λ_w	$T_{e,i}^{w}$
Gap between GST packet i and i + 1	g_i^w

Consider two GST packets inside the fusion node: GST packet i (GST i), a packet that arrives at the delay line and (GST i+1), another packet that is delineated in time after GST i.

1. At time t = $T_{a,i}^{w}$, figure 3.6 (a)

GST i arrives at the delay line. The arrival time of GST i ,$T_{a,i}^{w}$, to the output channel λ_w is updated to this time.

2. At time $t = T_{a,i}^{w} + T_{s,i}^{w}$, figure 3.6 (b)

The last bit of the GST i has entered into the delay line; the service time for this packet to enter to the delay line completely is $T_{s,i}^{w}$. At this time, the exit time of GST i is updated by adding δ, i.e. $T_{e,i}^{w} = T_{s,i}^{w} + T_{a,i}^{w} + \delta$,

After the last bit of GST i enters the delay line, we have two scenarios regarding the arrival of GST i+1; either it comes when GST i is still inside the delay line or after it gets out of the delay line.

i. If it arrives while GST i is still inside the delay line, this implies $T^w_{a,i+1} < T^w_{e,i}$, then the gap value (g^w_i) will be updated and passed to the scheduler as: $g^w_i = T^w_{a,i+1} - T^w_{e,i}$, figure 3.6 (c)

ii. If it arrives after GST i has exited the delay line, this implies $T^w_{a,i+1} \geq T^w_{e,i}$, then $g^w_i = \delta$, figure 3.6 (d)

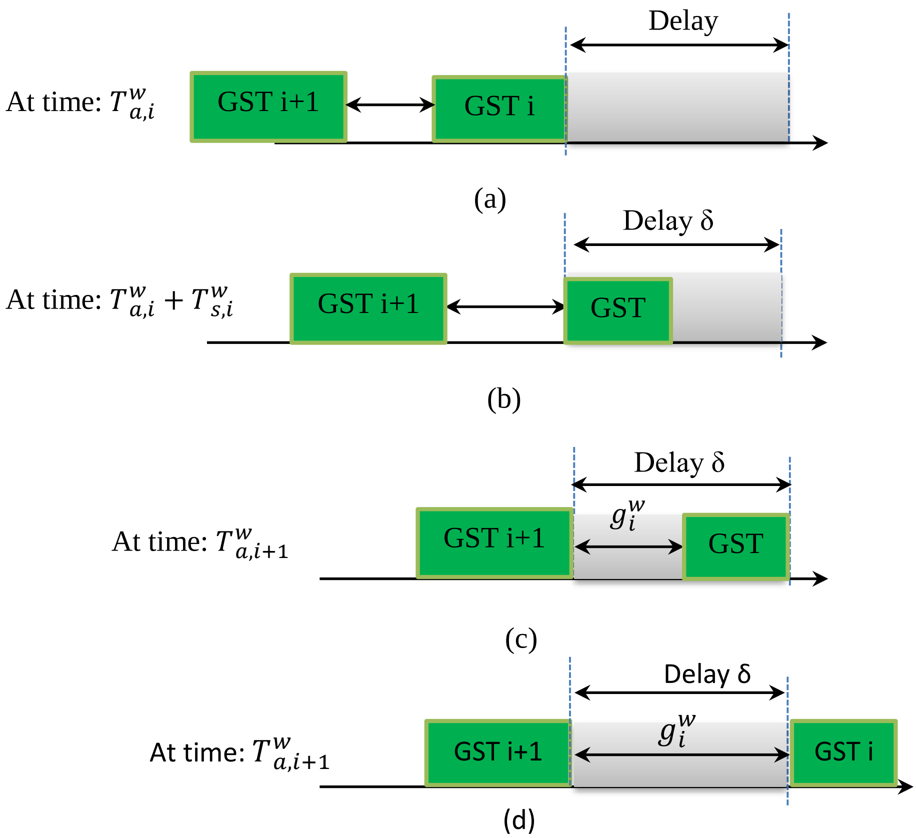

Figure 3.6 Detection of free time-gap between GST packets a) Packet i arrives at the delay line b) packet i completely enters the delay line c) packet i+1 arrives while packet i is still inside the delay line d) packet i+1 arrives after packet i left the delay line.

3.2 Sub-Wavelength Aggregation

In addition to adding SM traffic to increase the utilization of the provisioned GST wavelength, a virtual time-slotted scheme can be used to divide the provisioned GST wavelength into several sub-circuits. Dividing GST wavelength into timeslot enables aggregating multiple lower bit rate GST channel on a single GST wavelength, hence increase the capacity and decrease cost [26].

The use of this sub-wavelength aggregation scheme can be illustrated with the following example, and figure 3.7. Suppose several mobile stations are connected using metropolitan area network (MAN) that uses course wavelength Division multiplexing (CWDM) on different wavelengths.

Each wavelength can have a capacity of 10 Gb/s which is excess for mobile stations that require 1 Gb/s circuit channel. The capacity of the wavelength can be utilized in a more efficient way using time slots to aggregate multiple sub-wavelength traffic from different base stations; at the same time the aggregation scheme does not affect the circuit quality of the traffic. Moreover, the leftover capacity from the base stations can be used by connecting more customers using a router on the second 10 GE port of H1 node [27].

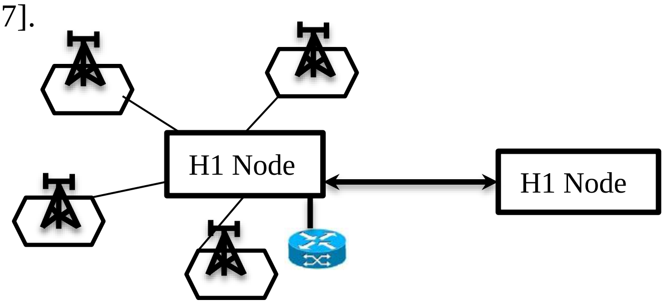

Figure 3.7 Sub-wavelength aggregating of traffic from multiple base stations.

3.2.1 Method of GST aggregation

Packet traffic between two end nodes (Ingress and Egress) can have one or multiple paths with one or more intermediate nodes.

When optical circuit switching is use, each path will have its own wavelength. However, with fusion nodes one or more GST streams can be aggregated on single wavelength by scheduling each GST stream on different time-slots. The GST streams will have a circuit QoS and bypass intermediate nodes, however if SM packets are added on the ingress node they will be dropped and queued [26].

While these streams of aggregated GST packets are traveling from sender to receiver on a light path, SM packets can be injected on the intermediate nodes if there is a gap on the light path. It is important to note here that adding traffic on the intermediate node does not affect the circuit QoS of the GST stream.

3.2.2 GST aggregation inside H1 node

Data containers are used in fusion node to aggregate and send one or more GST packets together with container control information**.** Container control information is used at the receiver node to learn about the GST packets, for example the source and destination address, the container's length, etc.

In order to illustrate the aggregation scheme in H1 nodes with example, five GST input streams on ports (ge 5 – ge 9), and one SM input on Xe port (Xe0) are used on figure 3.8. The second Xe port (Xe1) is used as an output port.

As can be seen from the figure, data received at the interface is identified as GST and SM packet based on a VLAN-tag, then the SM traffic is dropped at the SM DMUX for additional processing

While the dropped SM traffic stays in a queue and processed according to header information, the GST traffic bypasses the packet switch. After that, the GST traffic will be compressed in time to be sent out on the 10 GE interface. Here, the compression factor is the ratio of the 1 Gigabit/s to the 10 Gigabit/s, hence tenth. This implies the node has a potential of aggregating ten 1 Gigabit/s inputs into one 10 Gigabit/s output stream. If the data rate of incoming data is different on different inputs, then different time compression schemes can be used [26].

When GST packets reaches the delay line, the GST gap detector measures the gaps between the compressed GST packets and containers to be pass it to the SM packet scheduler.

The SM packet scheduler will then scan for SM packets, inside the queue, that can fit the measured gap between GST packets, and insert packets with fitting length; this increase the utilization of the light path. Before gaps are filled with the SM packets, the aggregated GST traffic should pass through a fixed amount of delay equivalent to the maximum SM length; this prevents pre-emption of SM packets.

At the receiving node, the inverse time compression factor is used to the aggregated packets. Therefore inter packet timing variation will be preserved with the same stream of data.

The discussion we made on sub-wavelength aggregation is similar to the discussion we made on section 3.1.2 with one important note to make. The first explains the operation of the H1 node when adding SM traffic on a vacant gap between GST packets of a single wavelength, and the second discusses aggregation of GST steam using sub-wavelength, and injection of SM packet between vacant gaps.

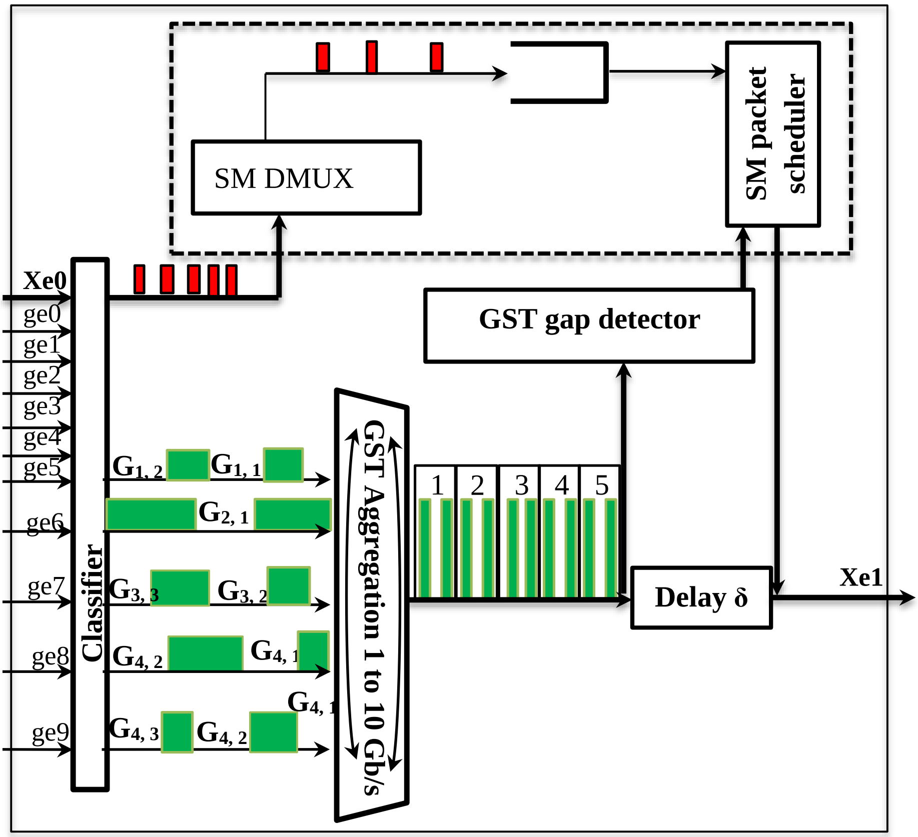

Figure 3.8 Internal operation of fusion node aggregating scheme; the figure is used to explain how the fusion node aggregate GST traffic, and inject SM traffic; it is depicted with five 1 GE input ports (ge 5 – ge10) as GST ports (green packets), and one Xe input port (Xe0) as SM (red packets). The second Xe port (Xe1) is used as an output port.

3.3 Related Work

In this section previous experiments that has been done to study fusion network performance is discussed. On the first part, we will present works done to utilize vacant gaps between GST packets by injecting SM packets. On the second part, previous experiment on sub-wavelength aggregation scheme will be discussed.

3.3.1 SM injection

A series of performance measurement on fusion nodes from TransPacket has been done at the Norwegian University Science and Technology (NTNU) through the carrier network of UNINETT by Veisllari et al. in [24]; they have presented two field-trial experiments, on a metro and long haul network.

Both experiments have shown that:

1. A guaranteed performance of GST with circuit QoS, i.e. irrespective of the added/dropped SM traffic.
2. An increase in light path utilization due to the added SM traffic, and

To further strengthen the experimental results, Edgar Sanchez and Kefu He [28], [29] have also performed the same experiment with different SM and GST configuration. Similar result with [24] was found proving the design principles of the fusion node in providing a circuit QoS for GST traffic, and a boost in resource utilization because of the interjected SM traffic.

3.3.2 Sub-wavelength aggregation

S. Bjørnstad, , et al. [30] have performed an experiment to demonstrate the sub-wavelength aggregation capability of the fusion node; on the experiment two fusion nodes that are 3.25 Km apart were connected by a 10 Gb/s wavelength light path. Five 1 Gb/s ports of Node 1 (N1) were used as an input for five GST streams which are aggregated into the 10 Gb/s output port; at the destination node, N2 each GST stream is de-aggregated into their corresponding ports. In addition to GST aggregation, an increasing amount of SM stream was added to the second 10 Gb/s port of N1, and inserted into the free-gaps between GST packet

Results from the experiment have shown that the inter-packet timing before and after aggregation was the same. GST traffic has shown low deterministic delay and no packet loss. Equally important, by adding SM stream on the free-gaps, it was possible to achieve higher throughput efficiency, and it has been proved there was no timing impact on the GST sub-wavelength.

On this thesis, the experiments we perform are made on a network setup similar to [30], however the nodes that are used to build the network are with an upgraded firmware, hence the result from this experiment are with fewer bugs than the results from [30]; In addition, the experiments done on this thesis are more extensive.

Three main tests were conducted with the aim of obtaining three performance metrics, i.e. PDV, PLR, Average packet lost.

The first experiment was performed by transmitting various loads of SM traffic on the network; the load on the 10 GE path was increased from 0.10 to 0.98 % to observe how different load of SM traffic is treated by the network.

The second experiment was done by transmitting an aggregated GST traffic through the network; we have varied the number of GST streams for different loads sizes. This experiment will help to observe the aggregating scheme in GST traffic.

Finally, on the third experiment we followed the same kind of scenario with the second experiment except, we have inserted SM traffic between gaps of aggregated GST packets. Doing so, we can observe:

1. The H1 nodes ability on aggregating circuit QoS GST traffic on sub-wavelengths, regardless of the SM traffic.

2. The increase in resource utilization that comes with injecting SM traffic on vacant light path.

Chapter 4

Methodology

The aim of this chapter is to describe the important components used on the experiment, the approach we take, and the experimental steps followed to perform the experiment. The first section focuses on the approach that we followed; the second section describes the hardware and software tools that are used on this thesis, and the final section discusses the test bed, and the experimental setup.

4.1 Approach

Among the three known scientific techniques of evaluating the performance of a network: simulation, experiment, and analytical modeling, on this thesis we followed the experimental approach.

The test-bed was set up at UNINETT with two prototype Fusion H1 nodes [25], and a remote management and configuration tools at NTNU. The first task was setting up a network that is built with H1 nodes; this network is used to study the performance of the nodes. Key performance metrics including packet delay variation, packet loss ratio, and end-to-end delay were extracted from several experiments.

Figure 4.1 below illustrates the network environment that was used for our performance test. It incorporates both UNINETT and NTNU. At NTNU, a desktop computer was used to configure and manage network equipment found at UNINETT.

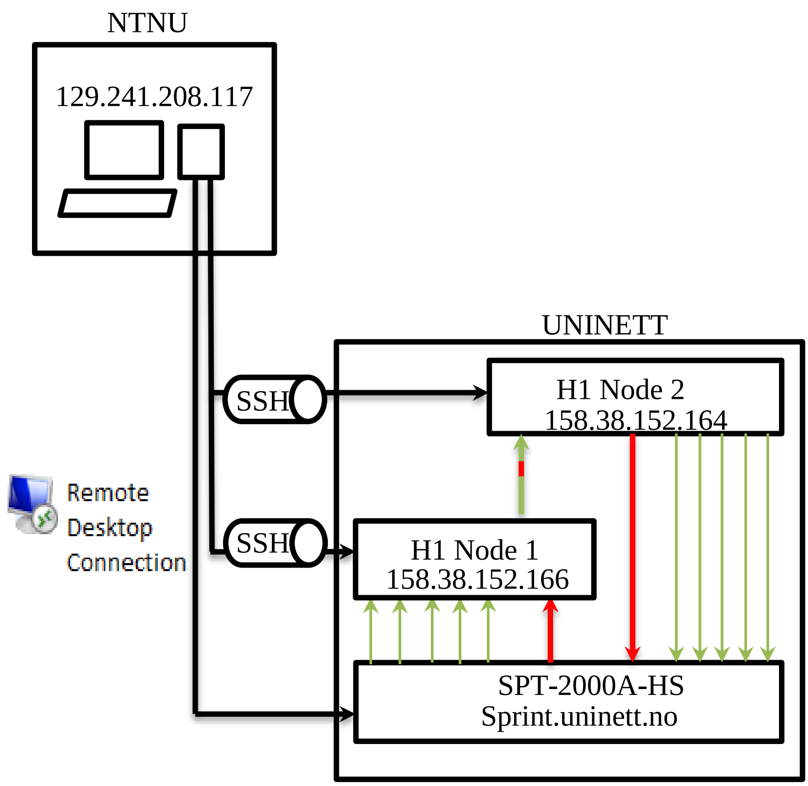

Figure 4.1 Network setup between UNINETT and NTNU; communication between desktop computer and the two H1 nodes was using SSH, and the communication between desktop computer and the SPT-2000A-HS through Remote Desktop connection.

UNINETT is the palace where the two H1 nodes, the main subjects of study, and a Spirent generator and analyzer, are located.

The management and configuration console at NTNU and the Spirent device at UNINETT were connected by Windows remote desktop functionality. In addition, Secure Shell (SSH) was used to connect the console at NTNU to the H1 nodes at UNINETT.

4.2 Hardware and Software

Three main hardware devices with different software were used to perform the experiment, and collect the result. On this section, we will address the hardware and software components used on the experiment.

4.2.1 H1 node

Figure 4.2 shows the fusion node also known as H1 muxponder. It has ten 1 Gigabit Ethernet ports (1 GE) (ge0 – ge9) that are configured as access interfaces, and two 10 Gigabit Ethernet ports (10GE) (Xe0 and Xe1) which can be configured in either access interface or trunk interface. It also has two management ports: RS232 and Ethernet port, and power input port and Reset button [25].

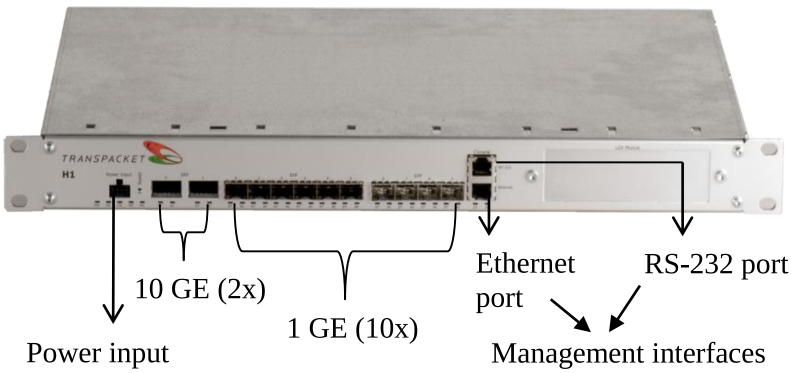

Figure 4.2 Illustration of H1 node's interface [25].

On this experiment two H1 nodes were used, one as a sender and the other as a receiver.

4.2.2 Spirent SPT-200A

Spirent SPT-200A is a device that is used to test performance of network nodes prior to deployment. It generates and transmits packets streams to the sender H1 node, and receives and analyzes packets that are coming from the receiver H1 node. On this thesis, we have used to generate and analyze packets [31].

Figure 4.3 Spirent SPT-200A [31].

The software installed on this device is called Spirent application test center; it has a graphical user interface where users can configure different parameters on the generated packets, streams, interfaces, and gather and analyze the results for different performance metrics. The PDV, PLR, and e2ed are the most important performance metrics that are extracted from the Spirent test center packet analyzer. It has a measurement timestamp resolution of 10 ns [32].

4.2.3 Personal computer

For remote configuration and data collection, a computer with Windows 7 operating system at NTNU was used. Putty, an open source terminal emulator, was used to make SSH connection with the two H1 nodes. In addition, Windows Remote Desktop connection functionality was utilized to connect to the sprint device remotely.

4.3 Test bed and Experimental description

The network setup at UNINETT set with the two H1 nodes, one configured as sender – H1 node 1 (N1) - and the other as receiver – H1 node 2 (N2), together with the Spirent nodes is depicted in figure 4.4.

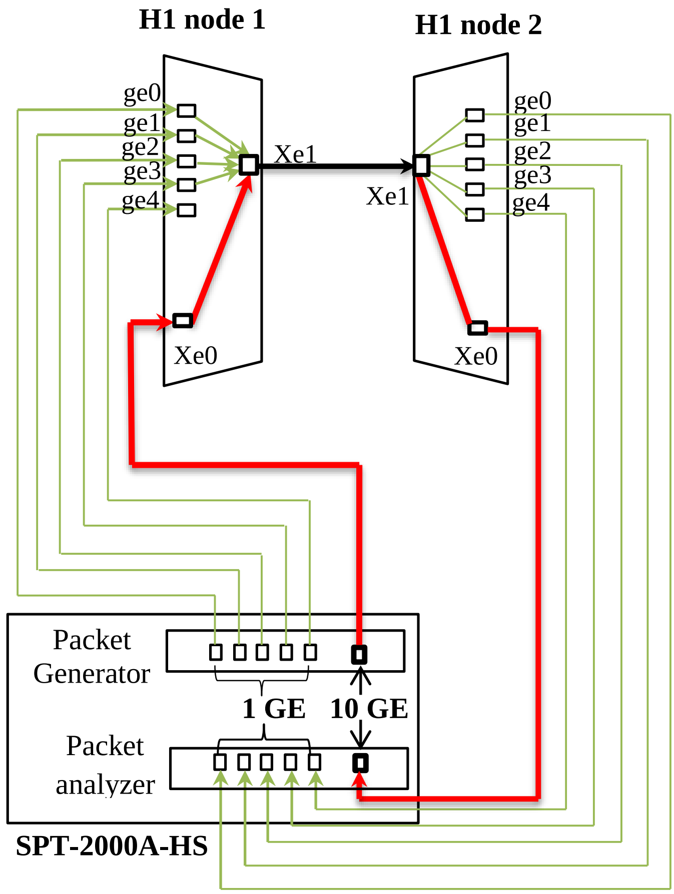

Figure 4.4 Port connection and traffic flow in the experiment network setup.

Figure 4.4 is not an exact representation of the H1 node and Spirent device; instead, we plot this diagram to ease the explanation of the test.

H1 nodes have ten 1 GE, and two 10 GE ports; however on this experiment five of the 1 GE ports were configured as sending and receiving GST ports on N1 and N2 respectively. One of the 10 GE ports on N1 and N2 was used as sending and receiving SM traffic, respectively.

Furthermore, the other 10 GE port was configured as an input port for N2 and output port for N1.

Likewise regardless of the number of ports on the Spirent devices only ten 1 GE and two 10 GE ports were used. As show in figure 4.4, five 1 GE ports, and one 10 GE port from the Spirent device is shown as packet generator. Another five ports 1 GE and one 10GE port were configured as packet analyzer. Ports are not logically divided as generator and analyzer on sprint device; the figure is plotted to elaborate the experiment.

During the experiment packets generated from the Spirent device are received on the input ports of N1. Five of the 1 GE packet streams received on the 1 GE port of the N1 are treated as GST traffic. Similarly, the 10 GE packet stream generated at the Spirent device is received at the 10GE port of the N1 and treated as SM traffic. After the received GST traffic on N1 is aggregated, and unutilized bandwidth is filled with SM traffic, it will be transmitted on the second 10 GE port of N1 to N2.

N2 receives the incoming traffic on the 10 GE input port and de-aggregate it to the respective ports. The output is, then, sent to the Spirent box for further analysis.

Chapter 5

Result

This Chapter will summarize the result gathered from the experiment made on the network setup presented on Chapter 4. Each section, 5.1 – 5.3, presents the performance of H1 node when transporting different traffic types: first SM traffic, second aggregated GST traffic, and finally the combination of both SM and aggregated GST traffic. Packet delay variation, packet loss ratio, and end-to-end delay were used to evaluate performance of the H1 node.

In addition to that, on the final sub-section, we have made an experiment to measure the maximum amount of SM that can be injected on a sub-wavelength aggregated GST traffic and a wavelength GST traffic.

Table 5.1 shows list of notations used for: different traffic loads on different interfaces, and delay components.

For the first two sections, the total load is equivalent to the loads of the traffic type used, either GST or SM. Therefore, for the first section $L^{T}_{10GE} = L^{SM}_{10GE}$, and for the second section $L^{T}_{10GE} = L^{GST}_{10GE}$. However on the third sub-section the total load will be the summation of SM and aggregated GST traffic, i.e. $L^{T}_{10GE} = L^{SM}_{10GE} + L^{GST}_{10GE}$

Table 5.1 List of notations for load values and delay components used in performance parameter calculation.

Load of SM traffic on 10 Gb/s interface	L_{10GE}^{SM}
Load of GST traffic on 1 Gb/s interface	$\mathrm{L}_{\mathrm{GE}}^{\mathrm{GST}}$
Total load of aggregated GST traffic on the 10 Gb/s interface	$\mathrm{L}_{\mathrm{10GE}}^{\mathrm{GST}}$
Total load (SM and GST) on the 10 Gb/s link	$\mathrm{L}_{\mathrm{10GE}}^{\mathrm{T}}$
Transmission delay	D(Tx)
Transmission delay of SM on 10 Gb/s link	$\mathrm{D(Tx)}\ _{\mathrm{10GE}}^{\mathrm{SM}}$
Propagation delay	D(Prop)
Propagation delay of SM on 10 Gb/s link	$\mathrm{D(Prop)}\ _{\mathrm{10GE}}^{\mathrm{SM}}$
Nodal delay	D(nod)
Nodal delay of SM on 10 Gb/s link	$\mathrm{Dnod)}\ _{\mathrm{10GE}}^{\mathrm{SM}}$
Transmission delay of GST on 1 Gb/s link	$\mathrm{DTx)}\ _{\mathrm{GE}}^{\mathrm{GST}}$
Total GST transmission delay	$\mathrm{D(Tx)}\ _{\mathrm{10GE}}^{\mathrm{GST}}$
Nodal delay of GST on 1 Gb/s link	$\mathrm{D(nod)}\ _{\mathrm{GE}}^{\mathrm{GST}}$

5.1 SM traffic performance

In order to observe how H1 node perform while transporting different SM traffic load (varied in the range 0.1 to 0.98), we have generated, transmitted and analyzed a 10 Gb/s SM stream between two H1 nodes; the generation and analysis part was done on a Spirent device.

- Right at the start, generated SM traffic from the Spirent device was sent to the 10 GE (Xe0) port of the first H1 node, N1;
- It is processed there and sent out to the second H1 node, N2, on the second 10 GE port (Xe1).

- Finally, the incoming SM traffic on the 10 GE (Xe1) port of N2 is processed, and sent to the Spirent device for performance analysis; experimental setup is depicted on figure 5.1.

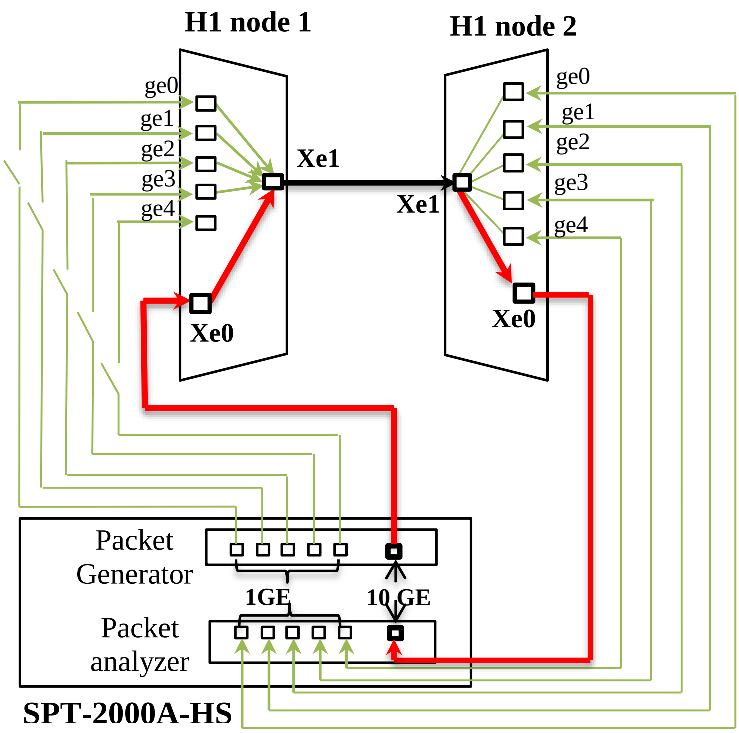

Figure 5.1 Network setup used to measure SM traffic performance; although 1 GE ports from Spirent device and N1 remains connected, we have drawn it open to show the absence of traffic flow.

SM traffic path

The Average e2ed, PLR, and PDV for the range of SM traffic load are discussed in the coming sub-sections.

5.1.1 Average end-to-end delay

The data on table 5.2 and the resulting graph, graph 5.2, shows the average e2ed SM traffic experience while traveling through the fusion network.

The average e2ed increases from 4.256 μs to 5.138 μs when the total load, L_{10GE}^{T}, was increased from 0.1 to 0.8 with an increasing interval of 0.1. However, when we increase L_{10GE}^{T} to 0.872, the end-to-end delay rise up to 27.39 μs.

Increasing more traffic, after 0.872, will cause a queue overflow, this increase the average e2ed exponentially and draws the network into a saturation state.

Table 5.2 Average e2ed for the respective load size of SM traffic.

No.	$\boldsymbol{L_{10GE}^{T}}$	**Average e2ed (μs)**
1	0.1	4.256
2	0.2	4.256
3	0.3	4.264
4	0.4	4.304
5	0.5	4.399
6	0.6	4.592
7	0.7	4.79
8	0.8	5.138
9	0.872	27.39
10	0.873	29 857.4
11	0.9	30 588.874
12	0.95	30 722.08
13	0.98	30 574.413

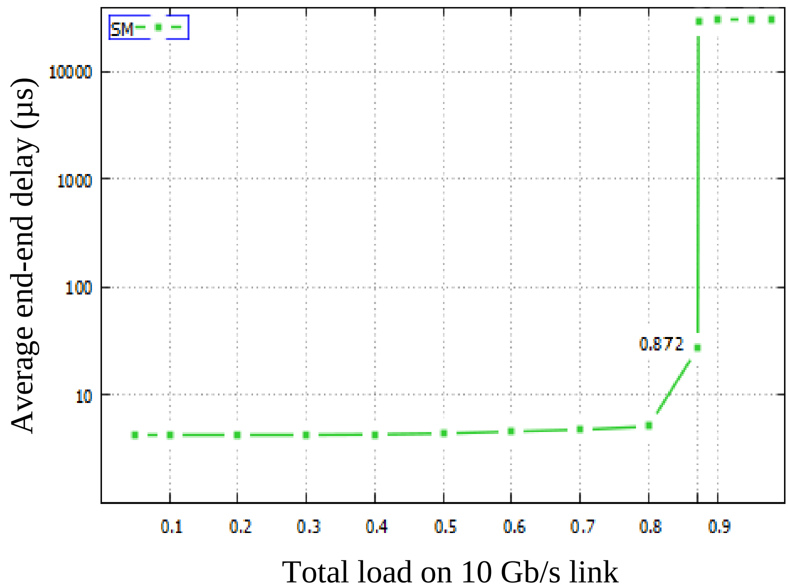

Figure 5.2 Average e2ed with respect to the total SM traffic load.

As discussed on chapter 2, the average e2ed can be divided into four main delay components, i.e. transmission, propagation, processing, and queuing delay. The transmission delay is the time it takes to put a packet from a node on to link; once the packet is on the transmission link it propagates to the destination node with a propagation time called the propagation delay. Inside a node, packets are processed and queued for the duration of time called processing and queuing delay respectively. Let us equate the combination of processing and queuing delay to the nodal delay, D (nod), this gives the e2ed as:

$$e2ed = D(Tx) + D(Prop) + D(nod) \qquad \ldots\ldots\ldots\ldots\ldots (1)$$

The transmission and propagation delay are dependent on the link capacity and distance respectively, and are almost constant for a specific type of network link [21].

5.1.1.1 Transmission delay

SM traffic encounter transmission delay when:

- SM traffic is send from the Spirent generator to N1 on a 10 Gb/s link,
- SM traffic is transmitted from N1 to N2 on the 10 Gb/s transmission link, and
- The second H1 node transmits the SM traffic to the Spirent analyzer on a 10 Gbs/s link.

Transmission delay can be calculated using the general formula stated at [21]:

$$D(Tx) = \frac{\text{packet length L (b)}}{\text{Bandwidth of the line (b/s)}} \quad \text{……..} \ (2)$$

In our experiment, the packet length for the SM stream was uniformly distributed between 64 and 1518 bytes; therefore, the average packet length was 791 bytes, and because the SM stream was transmitted on a 10 Gb/s line, the transmission delay can be calculated using (2) as:

$$D(Tx)\ {}^{\mathrm{SM}}_{10\mathrm{GE}} = \frac{791\mathrm{x}\ 8\ \mathrm{bits}}{10\,\frac{\mathrm{Gb}}{\mathrm{s}}} + \frac{791\mathrm{x}\ 8\ \mathrm{bits}}{10\,\frac{\mathrm{Gb}}{\mathrm{s}}} + \frac{791\mathrm{x}\ 8\ \mathrm{bits}}{10\,\frac{\mathrm{Gb}}{\mathrm{s}}}$$

$$D(Tx)\ {}^{SM}_{10\mathrm{GE}} = 1.8984\ \mu s$$

5.1.1.2 Propagation delay

Propagation delay is given by the general formula [21]:

$$D(Prop) = \frac{\text{End} - \text{to} - \text{end length (m)}}{\text{speed of light in fiber} \left(\frac{\mathrm{m}}{\mathrm{s}}\right)} \quad \text{……………} \ (3)$$

The two H1 nodes are connected with a short fiber link of an approximate length 1.2 m, and the refractive index (n) of light in glass is 3/2 [33], therefore approximately the velocity (V = C/n) of light in fiber is 2/3 C; where C is the speed of light, using equation (3):

$$D(\text{Prop})\,{}^{\text{SM}}_{10GE} = \frac{1.2\text{m}}{\frac{2}{3}C} = \frac{1.2\text{m}}{\frac{2}{3}299000000\frac{\text{m}}{\text{s}}}$$

$$D(\text{Prop})\,{}^{\text{SM}}_{10GE} = 6.02\text{ ns} \quad \ldots\ldots\ldots..\ (4)$$

5.1.1.3 Nodal delay

The remaining delay components are queuing and processing delay; as we have discussed above nodal delay was equated with the combination of processing and queuing delay.

From the experiment, for SM traffic load ranging from 0 to 0.8, we have found a minimum 4.256 µs and maximum 5.138 µs e2ed. We have also calculated the transmission and propagation delay using their respective general formula above.

Substituting these values on equation (1) the minimum nodal delay can be calculated as:

$$4.256\ \mu\text{s} = 1.8984\ \mu\text{s} + 6.02\text{ ns} + \text{minimum D (nod)}$$

$$\text{Minimum D(nod)}\,{}^{\text{SM}}_{10GE} = 2.3576\ \mu\text{s}$$

Likewise, the maximum nodal delay can be calculated as:

$$5.138\mu\text{s} = 1.8984\ \mu\text{s} + 6.02\text{ ns} + \text{maximum D (nod)}$$

$$\text{Maximum D(nod)}\ {}^{\text{SM}}_{10GE} = 3.2396\ \mu s$$

Since SM traffic is treated in the H1 node as packet switched traffic, the maximum and minimum nodal delay, 2.3576 μs and 3.2396 μs respectively are the result from queuing and processing of packets.

5.1.2 Packet loss ratio

The packet loss ratio is calculated by dividing the number of lost packets to the total transmitted packet.

Table 5.3 Average PLR for the respective load size of SM traffic.

No.	L^{T}_{10GE}	**PLR**
1	0.1	0
2	0.2	0
3	0.3	0
4	0.4	0
5	0.5	0
6	0.6	0
7	0.7	0
8	0.8	0
9	0.872	0
10	0.873	0
11	0.9	0.0000029
12	0.95	0.019
13	0.98	0.059
14	0.1	0.082

As has been noted on table 5.3 and figure 5.3, SM packets start getting dropped when the total load reaches 0.873. From that point on wards queue overflow will increase the loss exponentially, and takes the network into saturation.

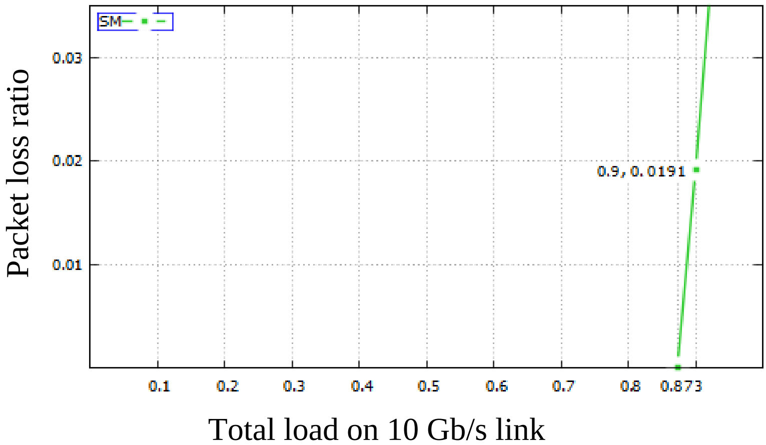

Figure 5.3 Average PLR with respect to the total SM traffic load

5.1.2 Average packet delay variation

The average PDV has constantly decreased when the load of SM traffic increased from 0.1 to 0.98 with minimum registered value 0.075 µs, and maximum registered value 0.682 µs. The result is tabulated and plotted in figure 5.4 and table 5.4 respectively.

Table 5.4 Average PDV for the respective load size of SM traffic.

No.	L_{10GE}^{T}	**Average PDV (µs)**
1	0.1	0.682
2	0.2	0.683
3	0.3	0.671
4	0.4	0.636
5	0.5	0.559
6	0.6	0.427
7	0.7	0.312
8	0.8	0.205
9	0.872	0.1300
10	0.873	0.1300
11	0.9	0.111
12	0.95	0.080
13	0.98	0.075

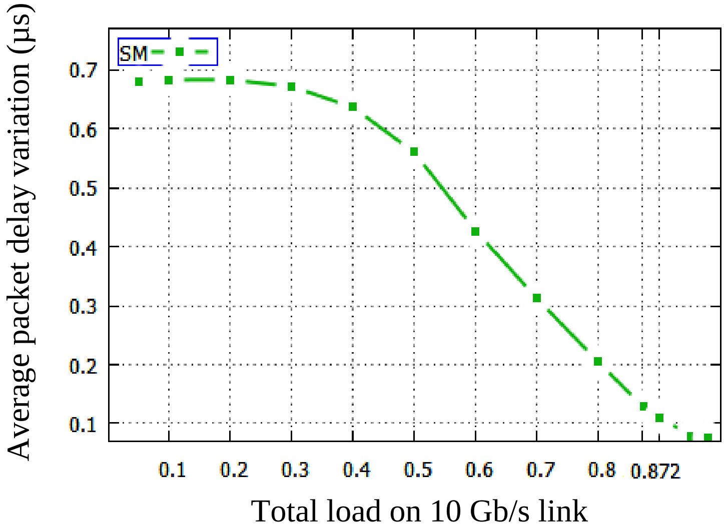

Figure 5.4 Average PDV with respect to the total SM traffic load

5.2 GST aggregation traffic performance

On the second experiment, we have observed the performance of the fusion node when transporting five aggregated 1 Gb/s sub-wavelengths GST streams on a single 10 Gb/s wavelength. The experiment was conducted by changing the total load of aggregated GST traffic, $L_{10GE,}^{GST}$ from 0.1 – 0.5, and the number of GST streams used to supply the total load was also varied from one to five; for each load size, each stream contributes an equal amount of load. On the experiment:

- Generated GST streams from the Spirent device were sent to the 1 GE (Xe0) ports of the first H1 node, N1;
- Received GST streams are aggregated, processed and sent out to the second H1 node, N2, on the 10 GE port (Xe1).
- Finally, the incoming GST traffic on the 10 GE (Xe1) port of N2 is de-aggregated, processed and sent to the Spirent device for performance analysis; experimental setup is depicted on figure 5.5.

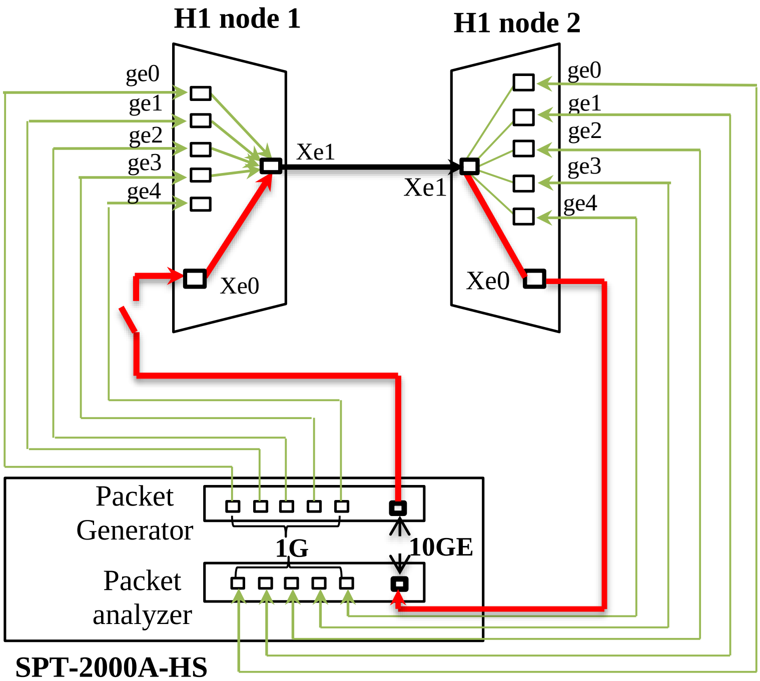

Figure 5.5 GST traffic performance measurement experiment setup; the SM link was opened to show absence of traffic flow.

GST traffic path

The Average e2ed, PLR, and PDV for the range of GST streams and corresponding load size, are presented in the coming sub-sections.

5.2.1 Average end-to-end delay

Table 5.5 and figure 5.6 shows the result of the average e2ed for the GST aggregation experiment; the measured experimental values for all cases lie in the range 50.97 µs to 51.02 µs.

Table 5.5 Average e2ed for the respective load size and number of GST streams. Total load on the 10 Gb/s link (TL), and Number of GST streams (NGS).

NGS / TL	1	2	3	4	5
0.1	50.988	50.986	51.00	51.020	51.018
0.15		50.970	50.99	51.011	51.012
0.2		50.980	50.97	51.002	51.008
0.25			50.97	50.980	51.000
0.3			50.98	50.978	50.980
0.35				50.9793	50.977
0.4				50.9873	50.976
0.45					50.978
0.5					50.986

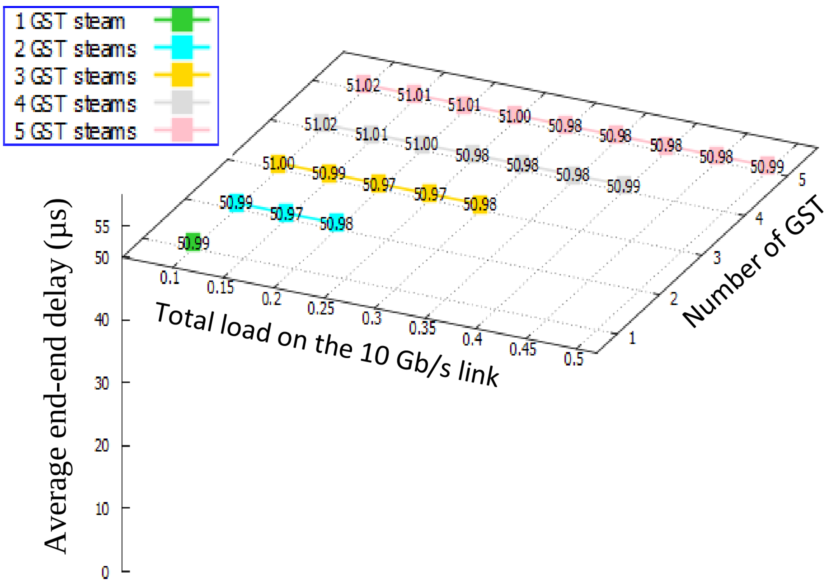

Figure 5.6 Average e2ed, load size, and number of GST traffic

With similar argument given on experiment one; we can divide the average e2ed into three delay components: transmission, propagation, and nodal delay.

5.2.1.1 Transmission delay

The aggregated GST traffic encounters transmission delay when:

- GST traffic is send from the Spirent generator to N1,
- Aggregated GST traffic is transmitted on the 10 Gb/s transmission link from N1 to N2, and
- The N2 transmits individual GST streams to the Spirent analyzer.

Therefore, the total transmission delay for the aggregated GST traffic can be calculated using:

$$\mathrm{D\ (Tx)}\ {}^{\mathrm{GST}}_{\mathrm{10GE}} = \mathrm{D(Tx)}\ {}^{\mathrm{GST}}_{\mathrm{GE}} + \mathrm{D(Tx)}\ {}^{\mathrm{GST}}_{\mathrm{10GE}} + \mathrm{D(Tx)}\ {}^{\mathrm{GST}}_{\mathrm{GE}} \quad \ldots\ldots\ldots (5)$$

The transmission delay is calculated using the same equation (2); however, while the average packet length of the aggregated GST traffic is similar with SM traffic (791 bytes), the link bandwidth used to transport the aggregated GST traffic is different from the link bandwidth that was used to transmit the SM traffic.

Individual GST streams generated from the Spirent device are transmitted on a 1 Gb/s link, thus:

$$\mathrm{D(Tx)}\ {}^{\mathrm{GST}}_{\mathrm{GE}} = \frac{791\mathrm{x}\ 8\ \mathrm{bits}}{1\frac{\mathrm{Gb}}{\mathrm{s}}} = 6.328\ \mu\mathrm{s}$$

, and for the GST streams transmitted on the 10 Gb/s transmission link:

$$\mathrm{D\ (Tx)}\ {}^{\mathrm{GST}}_{\mathrm{10GE}} = 0.6328\ \mu\mathrm{s}$$

Therefore, substituting these values to the total GST transmission delay given by equation (5):

$$D\ (Tx)\ _{10GE}^{GST} = \frac{791x\ 8\ bits}{1\frac{Gb}{s}} + \frac{791x\ 8\ bits}{10\frac{Gb}{s}} + \frac{791x\ 8\ bits}{1\frac{Gb}{s}}$$

$$D\ (Tx)\ _{10GE}^{GST} = \quad 13.2888\ \mu s \quad \ldots\ldots\ldots\ldots..\ (6)$$

5.2.1.2 Propagation delay

GST packets suffer the same amount of propagation delay as that of SM packets; therefore the propagation delay for GST traffic is 6.02 ns.

5.2.1.3 Nodal delay

The nodal delay for the aggregated GST traffic can be calculated using the same formula used for SM, equation (1).

As we have discussed on section 5.1.1, the GST traffic experience a minimum 50.97 µs and maximum 51.02 µs average e2ed. We can substitute the transmission delay from (5), and the propagation delay from (4) on equation (1) to calculate the minimum nodal delay.

$$50.97\ \mu s = \quad 13.2888\ \mu s + 6.02\ ns\ + \text{Minimum}\ D(nod)\ _{GE}^{GST}$$

$$\text{Minimum}\ D(nod)\ _{GE}^{GST} = \quad 37.6812\ \mu s$$

Similarly, the maximum nodal delay can be calculated as:

$$51.02\ \mu s = \quad 13.2888\ \mu s + 6.02\ ns + \text{Maximum}\ D(nod)\ _{GE}^{GST}$$

$$\text{Maximum}\ D(nod)\ _{GE}^{GST} = \quad 37.7312\ \mu s \quad \ldots\ldots.\ (7)$$

Unlike SM traffic, GST is treated in the H1 node with circuit quality; hence there is no queuing delay for GST traffic. While, the fixed delay δ that GST packets should go through accounts 7.68 µs, the remaining 30.0012 µs for the minimum and 30.0512 µs for the maximum nodal delay comes from processing delay.

5.2.2 Packet loss ratio

The experiment showed that every GST packet sent from the source was received at the other end; therefore the PLR of all GST traffic was zero.

5.2.3 Average packet delay variation

The result from GST aggregation shows that the average packet delay variation was very low; it lies within 0.032 µs to 0.0100 µs range.

Table 5.6 Average PDV for the respective load size and number of GST streams.

NGS / TL	1	2	3	4	5
0.1	0.012	0.030	0.019	0.015	0.032
0.15		0.020	0.030	0.030	0.031
0.2		0.010	0.022	0.030	0.012
0.25			0.023	0.015	0.030
0.3			0.012	0.021	0.031
0.35				0.032	0.031
0.4				0.012	0.029
0.45					0.025
0.5					0.012

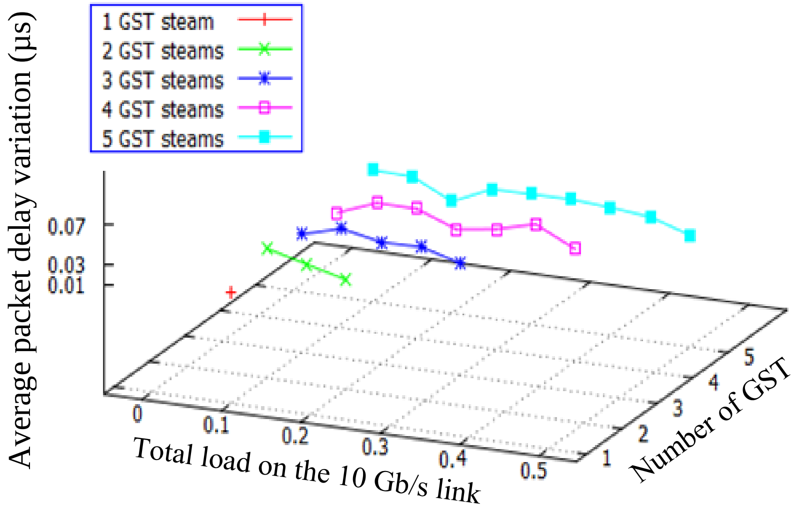

Figure 5.7 Average PDV, total load and number of GST.

5.3 GST aggregation and SM injection performance

The final experiment was done by transmitting five aggregated 1 Gb/s sub-wavelength GST streams on the single 10 Gb/s light path set between N1 and N2; the left over capacity from the light path was used to add SM packets. The network setup shown in figure 4.4 was used for this experiment.

The total load on the 10 Gb/s light path (L^{T}_{10GE}), from N1 to N2, is the combination of the total load from the aggregated GST traffic (L^{GST}_{10GE}) and the added SM traffic load (L^{SM}_{10GE}), hence $L^{T}_{10GE} = L^{GST}_{10GE} + L^{SM}_{10GE}$. In addition, the total load of the aggregated GST traffic, L^{GST}_{10GE}, is the sum of the loads from each GST traffic, L^{GST}_{GE}, each contributing equal amount, i.e. $L^{GST}_{10\,GE} = 5 * L^{GST}_{GE}$.

We will first present the maximum amount of SM traffic that was possible to add on the aggregated GST traffic, and then give the performance matrices gathered for different numbers of GST traffic used on the experiment.

5.3.1 Maximum SM traffic

We have varied the number of GST streams (NGS) from one to five for a range of L_{10GE}^{GST} (0.1 to 0.5), and registered the maximum amount SM traffic that can be added on the left over capacity.

Table 5.7 Maximum utilization of the 10 Gb/s link.

NGS / $\mathbf{L_{10GE}^{T}}$	**1**	**2**	**3**	**4**	**5**
0.1	0.857	0.7	0.723	0.713	0.714
0.15		0.677	0.614	0.628	0.638
0.2		0.673	0.586	0.529	0.534
0.25			0.577	0.497	0.445
0.3			0.575	0.484	0.409
0.35				0.478	0.392
0.4				0.477	0.384
0.45					0.38
0.5					0.379

Table 5.7 above shows the maximum utilization of the 10 Gb/s light path before SM packets starts dropping. The L_{10GE}^{GST} column shows the load of the aggregated GST traffic, the NGS row shows the number of aggregated GST streams, and the values in between are the maximum amount of added SM traffic.

When L_{10GE}^{GST} was equal to 0.5 with five 1 Gb/s GST traffic, it was possible to add a maximum load of 0.379 SM traffic. This implies the maximum utilization of the 10 Gb/s light path for this case was 0.879 (87.9%).

Another important observation was, when the load of the added SM traffic exceeds 0.379, SM packets start getting dropped due to packet switch queue overflow. However the GST traffic never showed a change in characteristic with the added SM traffic.

Five scenarios based on the number of aggregated GST streams will be discussed below.

5.3.2 One GST stream

Table 5.8 Load size, average PDV, average PLR, and average e2ed for one GST stream and SM traffic.

Load		**Average PDV**		**Average PLR**		**Average e2eD**	
L_{10GE}^{GST}	L_{10GE}^{SM}	**SM PDV**	**GST PDV**	**SM PLR (%)**	**GST PLR**	**SM e2ed**	**GST e2ed**
0.1	0.800	0.21	0.03	0	0	5.381	51.02
	0.850	0.16	0.03	0	0	8.297	51.02
	0.856	0.15	0.03	0	0	26.230	51.02
	0.857	0.15	0.03	1.4e-06	0	15,853.3	51.03

On the first scenario, we have used one 1 Gb/s GST stream with, $L_{10GE}^{GST} = L_{GE}^{GST} = 0.098$, and added an increasing SM traffic load.

As depicted in table 5.8, we have observed a drop in SM traffic, when the total load reaches, $L_{10GE}^{T} = L_{10GE}^{GST} + L_{10GE}^{SM} = 0.957$.

Until that point, the average SM PDV, and e2ed have stayed low, and there was no registered packet loss; however, when the total load passed 0.956, the packet loss, and the e2ed shows an exponential increase.

The GST traffic had almost stayed with a constant average e2ed 51.0245 µs, a constant average ultra-low average PDV 0.03 µs, and no packet loss.

5.3.3 Two aggregated GST streams

Table 5.9 Load size, average PDV, average PLR, and average e2ed for two GST stream and SM traffic

Total Load		**Total Average PDV**		**Total Average PLR**		**Total Average e2eD**	
$\mathbf{L_{10GE}^{GST}}$	$\mathbf{L_{10GE}^{SM}}$	**SM PDV**	**GST PDV**	**SM PLR**	**GST PLR**	**SM e2ed**	**GST e2ed**
0.1	0.700	0.41	0.03	0	0	510.44	50.99
	0.710	0.40	0.03	0.643	0	38,009.1	51.01
	0.720	0.39	0.03	1.656	0	38,030.3	51.01
	0.750	0.37	0.03	9.490	0	38,000.6	51.01
0.15	0.670	0.48	0.02	0	0	13.090	50.99
	0.677	0.47	0.02	0	0	103.940	50.96
	0.678	0.47	0.02	4e-03	0	38,533.3	50.95
	0.680	0.47	0.02	0.059	0	38,997.5	50.99
0.2	0.670	0.49	0.02	0	0	14.740	52.28
	0.673	0.48	0.01	0	0	56.860	50.97
	0.674	0.48	0.01	5e-04	0	37,520.6	50.97
	0.680	0.47	0.02	0.299	0	39,425.1	51.75

On the second scenario, two aggregated 1 Gb/s streams were used; the total aggregated GST traffic, $\mathrm{L_{10GE}^{GST}}$, was varied three times, 0.1, 0.15, and 0.2. For each case an increasing amount of SM traffic was added until we encounter a loss in SM packet.

For each $\mathrm{L_{10GE}^{GST}}$, the maximum amount of traffic load , $\mathrm{L_{10GE}^{T}}$, that was possible to transmit without SM packet loss was 0.87, 0.827, and 0.873 respectively.

SM traffic has shown the same behavior as that of the first scenario before and after packet loss encounter. The GST traffic also showed the same behavior with a constant average e2ed 51.1533 µs, and a constant ultra-low average PDV equals to 0.02083 µs.

5.3.4 Three aggregated GST streams

Table 5.10 Load size, average PDV, average PLR, and average e2ed for three GST stream and SM traffic.

Total Load		**Total Average PDV**		**Total Average PLR**		**Total Average e2ed**	
$\mathbf{L_{10GE}^{GST}}$	$\mathbf{L_{10GE}^{SM}}$	**SM PDV**	**GST PDV**	**SM PLR**	**GST PLR**	**SM e2ed**	**GST e2ed**
0.1	0.690	0.38	0.02	0	0	6.93	51.02
	0.723	0.34	0.02	0	0	134.360	51.01
	0.724	0.34	0.02	8e-03	0	36,182.6	51.01
	0.750	0.32	0.02	2.19	0	36,827.6	51.02
0.15	0.610	0.60	0.03	0	0	24.16	51.01
	0.614	0.59	0.03	0	0	97.55	50.99
	0.615	0.59	0.03	3e-03	0	40,917.3	50.99
	0.620	0.59	0.03	0.31	0	43,097.8	51.01
0.2	0.580	0.70	0.02	0	0	18.56	50.98
	0.586	0.68	0.02	0	0	140.25	50.98
	0.587	0.68	0.02	1e-02	0	44,361.2	50.98
	0.590	0.68	0.02	0.18	0	45,093.9	50.98
0.25	0.570	0.73	0.03	0	0	16.57	50.98
	0.577	0.72	0.03	0	0	113.74	50.96
	0.578	0.72	0.03	8e-03	0	44,877.1	50.96
	0.58	0.71	0.03	0.10	0	45,667.6	50.96
0.3	0.575	0.72	0.01	0	0	133.29	50.97
	0.576	0.72	0.01	1e-02	0	45,253.7	50.98

On the third scenario, the aggregated number of GST traffic has increased into three, the total aggregated GST traffic, $\mathrm{L_{10GE}^{GST}}$, was varied five times, 0.1, 0.15, 0.2, 0.25 and 0.3, and for each $\mathrm{L_{10GE}^{GST}}$ an increasing SM traffic load was added.

The maximum amount of traffic that was possible to transmit without SM packet loss for each L_{10GE}^{GST} was registered at 0.823, 0.764, 0.786, 0.827, and 0.875 respectively.

As of the two scenarios above SM traffic behaved on the same manner; the GST traffic kept being transported with constant average e2ed varying from 50.99 µs to 51.021 µs, and with a constant ultra-low average PDV varying from to 0.01 to 0.03 ns.

5.3.5 Four aggregated GST streams

Table 5.11 Load size, average PDV, average PLR, and average e2ed for four GST stream and SM traffic.

Total Load		**Total Average PDV**		**Total Average PLR**		**Total Average e2ed**	
$\mathbf{L_{10GE}^{GST}}$	$\mathbf{L_{10GE}^{SM}}$	**SM PDV**	**GST PDV**	**SM PLR**	**GST PLR**	**SM e2ed**	**GST e2ed**
0.1	0.710	0.36	0.02	0	0	16.60	51.02
	0.713	0.35	0.01	0	0	75.37	51.02
	0.714	0.35	0.01	7.4e-04	0	33,886.9	51.02
	0.720	0.35	0.02	0.323	0	37,215.6	51.02
0.15	0.620	0.51	0.01	0	0	19.27	51.01
	0.628	0.50	0.01	0	0	126.68	51.01
	0.629	0.50	0.01	0.003	0	39,467.3	51.01
	0.630	0.49	0.01	0.050	0	41,654.6	51.01
0.2	0.520	0.82	0.03	0	0	18.80	50.99
	0.529	0.80	0.03	0	0	140.59	50.99
	0.530	0.80	0.03	0.006	0	47,309.3	50.99
	0.590	0.72	0.03	6.957	0	50,023.5	50.99
0.25	0.490	0.95	0.02	0	0	21.53	50.97
	0.497	0.93	0.02	0	0	195.21	50.97
	0.498	0.93	0.02	0.022	0	52,214.9	50.97
	0.500	0.93	0.02	0.173	0	53,001.0	50.97
0.3	0.480	1.00	0.02	0	0	31.37	50.97
	0.484	0.99	0.02	0	0	247.48	50.97
	0.485	0.99	0.02	0.029	0	53,760.5	50.97
	0.490	0.98	0.02	99.500	0	54,722.9	50.97
0.35	0.470	1.04	0.03	0	0	18.53	50.96
	0.478	1.02	0.03	0	0	121.29	50.97
	0.479	1.02	0.03	0.005	0	52,770.0	50.97
	0.480	1.02	0.03	0.063	0	54,776.5	50.96
0.4	0.470	1.04	0.01	0	0	21.19	50.97
	0.477	1.02	0.01	0	0	323.41	50.99
	0.478	1.02	0.01	0.035	0	54,696.7	50.99
	0.480	1.02	0.01	0.193	0	55,286.2	50.97

On the fourth scenario, we aggregate four GST streams, and the L_{10GE}^{GST} was varied from 0.1 to 0.4 with 0.05 interval; on each of these total loads, we have added an increasing amount SM traffic load.

The same behavior similar to the above scenarios was observed here as well, until each $\mathrm{L}_{10\mathrm{GE}}^{\mathrm{T}}$ reached 0.813, 0.778, 0.729, 0.747, 0.784, 0.828, and 0.877 respectively, a low varying SM PDV, and e2ed was registered. Increasing more SM traffic will result in an exponential increases in loss and e2ed.

The average e2ed delay for the GST traffic was varying from 50.955 µs to 51.02 µs, with a constant ultra-low average PDV varying from to 0.01 µs to 0.03 µs regardless of the SM traffic load.

5.3.6 Five aggregated GST traffic

Table 5.12 Load size, average PDV, average PLR, and average e2ed for five GST stream and SM traffic.

Total Load		**Total Average PDV**	**Total Average PLR**			**Total Average e2ed**	
Load of GST	**Load of SM**	**SM PDV**	**GST PDV**	**SM PLR**	**GST PLR**	**SM E2ED**	**GST E2ED**
0.1	0.710	0.36	0.03	0	0	21.76	51.02
	0.714	0.35	0.03	0	0	188.32	51.02
	0.715	0.35	0.03	0.01	0	36,621.8	51.02
	0.720	0.35	0.03	0.29	0	37,173.0	51.02
0.15	0.630	0.47	0.03	0	0	15.950	51.01
	0.638	0.46	0.03	0	0	138.810	51.00
	0.639	0.46	0.03	9e-03	0	40,477.1	51.00
	0.640	0.46	0.03	0.05	0	41,122.3	51.02
0.2	0.530	0.70	0.01	0	0	51.360	51.01
	0.534	0.69	0.01	0	0	979.310	51.00
	0.535	0.69	0.01	0.06	0	48,919.9	51.00
	0.540	0.69	0.01	0.54	0	49,549.9	51.01
	0.440	1.03	0.03	0	0	38.480	51.00

0.25	0.445	1.02	0.03	0	0	325.730	50.99
	0.446	1.02	0.03	0.004	0	58,360.3	50.99
	0.450	1.02	0.03	0.49	0	59,357.2	50.99
0.3	0.400	1.22	0.03	0	0	23.280	50.97
	0.409	1.20	0.03	0	0	293.90	50.97
	0.410	1.19	0.03	0.04	0	63,358.3	50.97
0.35	0.390	1.29	0.03	0	0	63.840	50.97
	0.392	1.29	0.03	0	0	207.71	50.96
	0.393	1.28	0.03	0.02	0	65,604.9	50.96
	0.400	1.27	0.03		0	67,553.9	50.97
0.4	0.380	1.34	0.03	0	0	41.71	50.96
	0.384	1.33	0.03	0	0	481.65	50.97
	0.385	1.33	0.03	0.06	0	67,921.1	50.97
	0.390	1.32	0.03	0.6.9	0	68,950.8	50.96
0.45	0.380	1.35	0.02	0	0	338.96	50.97
	0.381	1.35	0.02	0.05	0	68,51	50.96
	0.390	1.33	0.02	1.283	0	69,788.9	50.97
0.5	0.370	1.38	0.01	0	0	22.10	50.98
	0.379	1.36	0.01	0	0	970.40	50.98
	0.380	1.35	0.01	0.07	0	69,024.1	50.98
	0.40	1.32	0.01	3.09	0	70,062.3	50.98

On the final scenario, five GST traffic were aggregate; the L_{10GE}^{GST} was increased from 0.1 to 0.5 with 0.05 increasing interval. In the same way we have done for the previous scenarios, we have increased the amount of SM traffic.

As expected, the SM traffic performed the same way as the previous scenarios, and the average e2ed for the GST traffic was varying from 50.964 µs to 51.02 µs with a constant ultra-low average PDV varying from to 0.01 µs to 0.03 µs.

The maximum amount of traffic that was possible to transmit without packet loss for this case was 0.814, 0.788, 0.734, 0.695, 0.709, 0.742, 0.784, 0.83, and 0.879, for each L_{10GE}^{GST}., i.e. 0.1, 01.5,0.2, 0.25, 0.3, 0.35, 0.4, 0.45, 0.5 respectively

5.4 Comparison between sub-wavelength aggregation and wavelength transport

On the last experiment we have run an experiment to compare the maximum amount of SM traffic that can be injected on GST wavelength with load 0.5, and the maximum SM traffic that can be inject on five aggregated sub-wavelength GST traffics with total load 0.5.

While table 5.13 shows the maximum amount of SM traffic that can be added to the GST traffic on the wavelength is 0.206, table 5.14 shows that the maximum SM traffic load that can be added to the aggregated GST traffic is 0.379.

Table 5.13 Maximum amount of SM traffic that can be added to wavelength GST traffic of load 0.5.

Total Load		**Total Average PDV**		**Total Average PLR**		**Total Average e2ed**	
Load of GST	**Load of SM**	**SM PDV**	**GST PDV**	**SM PLR**	**GST PLR**	**SM e2ed**	**GST e2ed**
0.5	0.206	0.23e04	0.03	0	0	1.7e4	23.11
	0.207	0.22e02	0.03	0.013	0	2.4e5	23.11

Table 5.14 Maximum amount of SM traffic that can be added to five sub-wavelength aggregated GST traffic with load 0.5.

Total Load		**Total Average PDV**		**Total Average PLR**		**Total Average e2ed**	
Load of GST	**Load of SM**	**SM PDV**	**GST PDV**	**SM PLR**	**GST PLR**	**SM E2ED**	**GST E2ED**
0.5	0.370	1.38	0.01	0	0	22.10	50.98
	0.379	1.36	0.01	0	0	970.40	50.98
	0.380	1.35	0.01	0.07	0	69,024.1	50.98
	0.40	1.32	0.01	3.09	0	70,062.3	50.98

Chapter 6

Discussion

On this chapter, we will discuss implication of results gathered from the experiment. On the first section, results are compared with recommended network performance values; the second section, discusses service differentiation in Statistical Multiplexed traffic; on third section, results from [30] are compared with result values from this thesis, to demonstrate how the firmware upgrade improve the performance of the H1 node. On the last section, we will discuss how much SM traffic can be added to five aggregated sub-wavelength GST streams with total load 5 Gb/s, and how much SM traffic can be added on a single 5 Gb/s GST wavelength, this comparison will aid how load balancing can be applied on the nodes for future work.

6.1 Performance metrics comparison with prior studies

We have gone through the recommended network performance metrics given by ITU-T's Network performance objectives recommendation paper [34] and other studies [35], and compared them with our experimental result; accordingly, we have come to a conclusion that supports TransPacket H1 node's design goal: supporting various network applications with the required service quality; moreover, increase link utilization.

ITU-T divides various network applications used on communication networks into six sets of network QoS classes; give different application examples, and the upper bound value for the network performance parameters as shown in table 6.1.

The recommendation [34] covers various applications such as conversational telephony, multimedia conferencing, digital video, and interactive data transfer. The upper bound values are given for a network range starting from the sending side, traversing through the network provider side and the inter-network links to the destination.

Table 6.1 ITU-T's recommendation of upper bound performance metrics for various applications, when the upper bound value is given as "U", it means sometimes poor quality is acceptable where given [34].

QoS class	**Applications (examples)**	**Network performance parameter (upper bound)**		
		IPTD	**IPDV**	**IPLR**
0	Real-time, jitter sensitive, high interaction (VoIP, VTC)	100 ms	50 ms	1 × 10–3
1	Real-time, jitter sensitive, interactive (VoIP, VTC).	400 ms	50 ms	1 × 10–3
2	Transaction data, highly interactive (Signaling)	100 ms	U	1 × 10–3
3	Transaction data, interactive	400 ms	U	1 × 10–3
4	Low loss only (short transactions, bulk data, video streaming)	1 s	U	1 × 10–3
5	Traditional applications of default IP networks	U	U	U

On our experiment we have aggregated five 1 Gb/s GST sub-wavelength streams from a source node and send it to the destination node on a 10 Gb/s link; in addition a 10 Gb/s SM traffic was injected on vacant gaps between GST packets

GST streams are meant to carry circuit quality traffic that is very sensitive to end-to-end delay, packet delay variation and packet loss ratio. Registered values from experiment show no packet loss for GST traffic. A controlled and low average e2ed with a maximum value 52.28 µs and a minimum value 50.95 µs, and an ultra-low PDV with maximum value 0.03 µs and minimum 0.01 µs were also registered. This result stayed constant for all cases independent of the added SM traffic.

Since our experiment was done in a network environment set inside one building, the nodes were not far enough to reflect what would have been true in real world network scenario. Therefore, let us extend the results from our experiment, and approximate how the fusion network performs if one node was deployed in Oslo and the other in Trondheim, with a one way distance around 500 km.

Even though it is difficult to give an approximation for the PLR and PDV (as this values are not directly related to distance), experiment from [24] done on a network set between Oslo and Trondheim have shown the value of PLR and PDV stayed unaffected with distance. However, due to the propagation delay, which increases with distance, it is clear that the average e2ed will have a significant difference from what we have found on our result.

The vast amount of delay for fiber communication comes from fiber latency encountered due to the refractive index of fiber that slows the speed of light approximately 5 μs per kilometer, and the other major contribution for latency is from a network Dispersion Compensating Fiber (DCF) component with a worst case scenario equals to 25% of the fiber delay [36]. Other components in a network contribute insignificant value to the total e2ed, therefore we have left them out from our approximation.

Using the approximation values, for a distance range from Oslo to Trondheim the fiber latency will be 5 μs/km x500km=2500 μs, and the latency from DCF will be 0.25x2500 μs = 625 μs; adding this values with the nodal and transmission delay encountered at the H1 node, will result in a total e2ed. We can use equation (1) from section 5.1.1:

e2ed = nodal delay + transmission delay + propagation delay

Substituting values from section 5.2.1.3 (7), maximum nodal delay is 37.7312 μs, the total transmission delay from section 5.2.1.1 (6) is 13.2888 μs, and together with our approximated calculation from fiber and DCF latency (625 μs + 2500 μs = 3125 μs), the one way delay from Oslo to Trondheim will be:

One way delay = 37.7312 μs + 13.2888 μs + 3125 μs

One way delay = 3176. 0192 μs

In addition to that, according to another study study [35], table 6.2 illustrates the requirements of delay-sensitive applications concerning one-way delay.

Table 6.2 Maximum one way delay required for various applications [35].

Application type	Maximum delay (one-way)
IPTV	<100 ms
Video-on-Demand	<50 ms
VoIP	<150 ms
Video Conferencing	<150 ms
Gaming	<50 ms

If we compare the values we get from our experiment, with every upper bound values given in ITU-T's recommendation and study made on [35], we can see that the performance metrics from fusion nodes is a lot less, approximately 3176.02 μs.

For the SM traffic, until the total load reaches the point where packets start dropping, the fusion node performs well in handling SM traffic. There was no registered loss, and the average PDV and e2ed was low.

6.2 Service differentiation

As we have discussed throughout the thesis SM traffic was presented as a traffic type with a low priority. Compared to the recommendations given in [34] and the study in [35], the SM traffic was lower than the upper bound parameters given for most of the service types. In addition to using the SM traffic as a general low priority traffic, it can be further differentiated across a range of applications with different QoS. The applications presented on table 6.1 and table 6.2 have different requirements in delay, loss, and PDV; these various requirements can be handled by service differentiation.

Such kind of approach has been demonstrated in 3-Level Integrated Hybrid Optical Network [37]. It extends OpMiGua by further dividing the traffic types into three: GST the highest priority traffic like the GST traffic type in OpMiGua, and two other packet switched types of traffic similar to the SM traffic in OpMiGua. One is SM/RT a packet switched type of traffic but with higher priority than the second SM type of traffic SM/BE.

6.3 Effective bandwidth utilization

Experiments done on [24] show the traffic pattern in today's network; the available bandwidth was not utilized fully for most of the time. On the same paper, two prototype H1 nodes were used on a network set between Oslo and Trondheim. A mirrored production traffic from UNINETT gateway router located in Trondheim was sent to the first 10 GE port of H1 node; this traffic was labeled as GST. In addition, they have generated and injected six 1 GE streams on the GST traffic to be sent to the second node at Oslo, this traffic was then looped back to Trondheim for analysis.

While the vertical axis on figure 6.1 represents the load of the GST traffic, the horizontal axis depicts the day format mm/dd/hh:hh (moth, date, hour). The green colored traffic load is for production traffic labeled as GST traffic, and the blue color for the injected SM traffic.

As can be seen, the link capacity was not utilized by the production traffic fully (green), and the paper demonstrates how it can be efficiently used by injecting SM traffic (blue) on it.

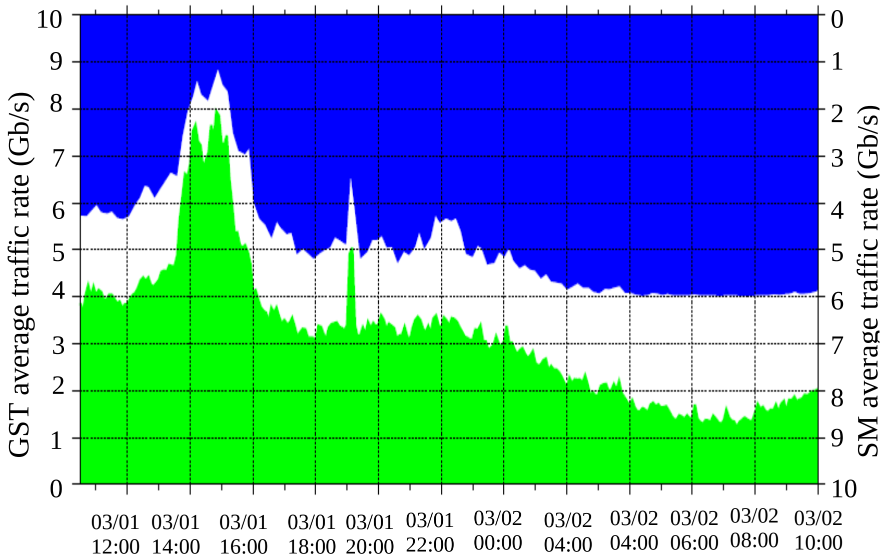

Figure 6.1 Load with respect to time of the day on the Trondheim – Oslo link; green represents load of GST traffic and blue for SM traffic [24].

The aggregation scenario is yet another scheme from H1 nodes to utilize the available wavelength with multiple aggregated sub-wavelength GST traffic, increase the efficiency of utilizing the available bandwidth, and reduce cost.

6.4 Comparison with prior work

Table 6.3 shows the maximum amount of utilization that was achieved from experiment [30]; comparing these values with the result found on our thesis, table 5.7, we can see how the firmware upgrade has resulted an increase in bandwidth utilization. For every aggregated GST stream, the amount of SM traffic that was able to add was higher on this thesis.

Table 6.3 Maximum utilization of the 10 Gb/s link from experiment [30].

Total GST load $\rho^T g$	Number of GST streams: g				
	1	2	3	4	5
0.1	0.72	0.656	0.684	0.672	0.668
0.15	-	0.641	0.570	0.523	0.603
0.2	-	0.621	0.554	0.492	0.457
0.25	-	-	0.5405	0.469	0.406
0.3	-	-	0.521	0.464	0.39
0.35	-	-	-	0.439	0.377
0.4	-	-	-	0.423	0.368
0.45	-	-	-	-	0.338
0.5	-	-	-	-	0.324

6.5 Comparison between sub-wavelength aggregation and wavelength transport

The result from section 5.4 shows transporting aggregated GST traffic allowed more SM traffic injection than injecting on GST wavelength. As shown in figure 6.2 and 6.3, this difference comes from the arrival rate of the SM traffic; on figure 6.2, SM traffic arrives on the 10 GE (Xe0) interface at a faster rate than the one shown on figure 6.3 - on the 1 GE interface. The faster packets arrive the faster scheduling is done, and the greater the number of SM packet scheduled on the gaps of the GST traffic in a given period of time, therefore this increases the total light path utilization.

Together with other studies, this result can be used for a load balancing scenario in fusion networks.

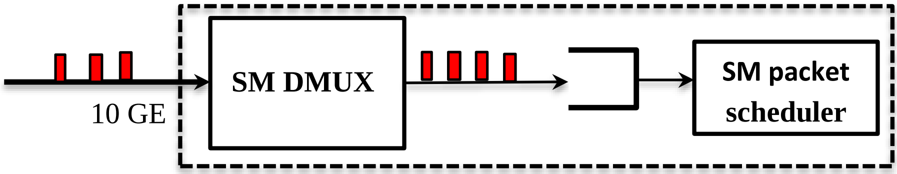

Figure 6.2 Experimental depiction of the SM traffic injection on the aggregated sub-wavelength GST traffic.

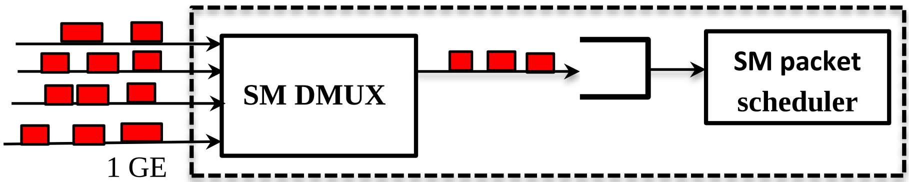

Figure 6.3 Experimental depiction of SM traffic injection on the wavelength GST traffic.

Results from all the experiment lead to a conclusion that indicate aggregating multiple fractional wavelength guaranteed performance traffic on a single wavelength and injecting addition SM traffic on vacant gap is possible in the fusion network.

Chapter 7

Conclusion

The growing number of new network applications and the demand for access towards these applications has increased the rate of internet traffic. In order to manage this demand, new technologies both in the optical and electrical fields are needed. Fiber optics offers a fat pipe of enormous bandwidth; in order to cope up with the huge data coming from this fat pipes, the switching devices should also offer greater speed. Furthermore, to increase performance of switches we have to be able to use resources efficiently.

Currently, the research work towards all optical switch is in research laboratories; however, it seems we have to wait more time until we see one in the real world. Therefore, until all optical switches become reality, a better way of switching our data is proposed by TransPacket as a hybrid switching node called Fusion H1 node. Fusion H1 node integrates the best qualities of the circuit and packet switched networks. This device treats traffic into two forms.

GST traffic is handled by the device with a deterministic QoS, the same way traffic is transported in a circuit switched network; moreover, the unutilized vacant gaps between GST packets are filled with a second type of traffic called SM traffic that is treated with packet switched network type of transport. Furthermore, the H1 nodes are capable of aggregating multiple circuit quality sub-wavelength GST traffic into single wavelength.

In this thesis the performance of fusion node in aggregating multiple sub-wavelength GST traffic, and utilizing the leftover capacity with SM traffic was studied. We have measured PDV, PLR and e2ed of both the aggregated GST and SM traffic to measure the performance of the H1 node; the results showed that properties of circuit and packet network was reflected on GST and SM traffic respectively.

In addition, recommendation from ITU-T and other study were considered for examining how networks should perform to provide the required service quality for customers. These recommendations were compared with the result gathered from our experiment made on the fusion network. The results demonstrate: the performance parameters achieved in the fusion network are lower than the upper bound parameters given on the recommendation and on the study.

For the most time sensitive applications which require high interactivity, class 0 applications (table 6.1), ITU-T recommends one-way upper bound packet delay of 100 ms, packet delay variation 50 ms and packet loss ratio of 1 x 10^{-3}. However, according to our experiment the worst case values from fusion node are much lower. Since our experiment was done inside a laboratory, we have tried to take into account the effect of distance and approximated the performance parameter value for Oslo – Trondheim range (500 km).

For a scenario where five 1 GE sub-wavelength GST streams were aggregated and SM traffic was injected on the left over capacity, the maximum one way delay for GST packet was approximately 3.176 ms. This is much lower than the ITU-T recommendation value for the most time sensitive and highly interactive application. Throughout the experiment, there was no GST packet loss, and the maximum registered PDV was 0.3 ns, which again are much better than what is recommended from ITU-T. These results indicate the performance of TransPacket H1 node has shown better result from what can be achievable in the conventional packet switched networks.

In general, the thesis has confirmed two important design concepts of H1 nodes:

(1) The H1 nodes ability to aggregate multiple sub-wavelength GST traffic on a single wavelength, keeping the deterministic characteristics of circuits: no packet loss, constant delay and ultra-low packet delay variation.

(2) Higher utilization of bandwidth by inserting SM traffic when there is gap between GST packets.

References

[1] Cisco white paper, “Cisco Visual Networking Index: Forecast and Methodology, 2012–2017,” May 2013.

[2] TRANSPACKET H1; a fusion networking add-drop muxponder, [Online]. Available: http://www.transpacket.com/wp-content/uploads/2011/12/TransPacket-H1-Product-overview-v1.pdf

[3] Fernández, P. M, “Circuit switching in the internet.” Ph.D. dissertation, Stanford University, 2003.

[4] F. Gebali, *Analysis of Computer and Communication Networks*. Springer, 2008.

[5] J. Walrand, and P. Varaiya, *High-performance communication networks*, 2nd ed., Morgan Kaufmann, San Francisco, 2000.

[6] CWDM and DWDM networking [Online]. Available: www.transpacket.com/wp-content/uploads/2011/07/Basic_WDM.pdf.

[7] IEEE Standard for Ethernet, IEEE Standard 802.3, 2012.

[8] Network node interface for the synchronous digital hierarchy (SDH), ITU-T Recommendation G.707/Y.1322, 2007.

[9] R. Ballart, and Yau-Chau Ching, “SONET: now it's the standard optical network,” Communications Magazine, IEEE, vol.27, no.3, pp.8-15, March 1989.

[10] Architecture of optical transport networks, Recommendation ITU-T G.872 A, 2012.

[11] S. Bjørnstad, M. Nord, T. Olsen, D. Hjelme, and N. Stol, “Burst, packet and hybrid switching in the optical core network”, TELEKTRONIKK, 2005.

[12] P. B. Chu, S. S. Lee, and S. Park, “MEMS: the path to large optical crossconnects,” IEEE Commun. Mag., vol. 40, pp. 80–87, Mar. 2002.

[13] M. Hoffmann, P. Kopka, and E. Voges, “Thermo-optical digital switch arrays in silica-on-silicon with defined zero-voltage state,” J. Lightwave Technol., vol. 16, pp. 395–400, 1998.

[14] H. Øverby, “Quality of Service Differentiation, Teletraffic Analysis and Network Layer Packet Redundancy in Optical Packet Switched Networks,” Ph.D. thesis, Norwegian Univ. of Sci. and Tech., June 2005.

[15] W. Stallings, *Data and computer communications*, Prentice Hall, 2007.

[16] Semeria, C. Multiprotocol Label Switching–Enhancing Routing in the New Public Network, White Paper, [Online]. Available: http://mirror.unpad.ac.id/orari/library/library-ref-eng/ref-eng-3/network/mpls/200001.pdf.

[17] D.V. Cunha, G. Bressan, “Generalized MPLS - an overview,” Telecommunications, 2003. ConTEL 2003. Proceedings of the 7th International Conference on , vol.2, pp.435-442 vol.2, June 2003.

[18] F. Masatti, P. Gavignet-Morin, D.Chiaroni, and G. Da Loura, “Fiber delay lines optical buffer for ATM photonic switching applications,” in Proc. IEEE Infocom, pp. 935–942, 1993.

[19] C.M. Gauger, J.P. Kuhn, E.V. Breusegem, M. Pickavet, and P. Demeester, “Hybrid optical network architectures: bringing packets and circuits together,” IEEE Communication. Magazine, vol.44, no. 8, pp. 36-42, 2006.

[20] M.Sadiku, Performance Analysis of Computer Networks, Springer, Jun 24, 2013.

[21] J.F. Kurose, and K.W. Ross, *Computer Networking: A Top-Down Approach Featuring the Internet*, 5th ed., Addison Wesley, 2010.

[22] Fusion networking explained [Online], Available: http://www.transpacket.com/wp-content/uploads/2012/06/White_paper_fusion_intro_12062012.pdf.

[23] S. Bjørnstad, D.R. Hjelme, and N. Stol, "A Packet-Switched Hybrid Optical Network with Service Guarantees," IEEE Journal on Selected Areas in Communications (Supplement on Optical Communications and Networking), vol. 24, no. 8, pp. 97–107, 2006.

[24] R. Veisllari, S. Bjørnstad, K. and Bozorgebrahimi, "Integrated packet/circuit hybrid network field trial with production traffic [invited]," Optical Communications and Networking, IEEE/OSA Journal of, vol.5, no.10, pp.A257-A266, Oct. 2013.

[25] Technical Guide H1, TransPacket, 2012.

[26] S. Bjørnstad, J.P. Braute, "Optical Switching", Patent Application WO2012104623A3, Jan 24, 2013.

[27] TransPacket Fusion Networking [Online], Available: http://www.transpacket.com/wp-content/uploads/2014/04/TransPacket-Fusion-networking-8p.pdf.

[28] E. G. Sanchez Gomez, "Fusion network performance experiment," M.Sc. thesis, Department of Telematics, Norwegian University of Science and Technology (NTNU), June 2013.

[29] He, K., "Fusion network performance experiment," M.Sc. thesis, Department of Telematics, Norwegian University of Science and Technology (NTNU), June 2013.

[30] S. Bjørnstad, R. Veisllari, J. P. Braute, and K. Bozorgebrahimi, “Integrated Packet/Circuit Hybrid Network Field-Trial Demonstrating Sub-Wavelength Aggregation,” In Optical Fiber Communication Conference, Optical Society of America, pp.W4-H.4, March 2014.

[31] Spirent TestCenter: SPT-2000A, SPT-5000A AND SPT-9000A CH-ASSIS [Online], Available: http://www.livingston-products.com/products/pdf/142602_1_en.pdf.

[32] 10-GIGABIT ETHERNET MULTIPLE MSA TEST SOLUTION [Online], Available: http://www.trs-rentelco.com/Specs-Manuals/SPRT_MSA-1001B_Spec.pdf.

[33] J. Laferrière, G Lietaert, R Taws, and S Wolszczok, Reference guide to fiber optic testing, 2011.

[34] Network performance objectives for IP-based services, Recommendation ITU-T Y.1541, 2011.

[35] J. D. Houle, K. K. Ramakrishnan, R. Sadhvani, M. Yuksel, and S. Kalyanaraman, “The evolving internet - traffic, engineering, and roles,” in Proc. of Research Conference on Communication, Information and Internet Policy (TPRC), Arlington, VA, September 2007.

[36] Low Latency – How low can you go? [Online], Available: http://www.transmode.com/en/resource/whitepapers?task=document.download&id=108.

[37] N. Stol, C. Raffaelli, M. Savi:”3-Level integrated hybrid optical network (3LIHON) to meet future QoS requirements”’, IEEE Globecom 2011, Houston, Texas, USA, Dec. 2011.